ński15

University of Crete-Physics Department

Undergraduate Thesis

Spectroscopic Classification of 20 candidate HMXBs in the Large Magellanic Cloud

Author:
Elias M. Kyritsis

Supervisor:
Prof. Andreas Zezas

September 18, 2019

Contents

1 Introduction

It was 1962 when a new era began for X-Ray astronomy. A team, under the superviion of Riccardo Giacconi, launched a rocket carrying a highly sensitive soft X-ray detector desinged by Frank Paolini,detected a significant emmision of soft X-rays that were not coming from the moon. This detection was the first extra-solar X-ray source Sco X-1 which lies in the constellation Scorpius (Giacconi et al. 1962)(3). Nearly 50 years after this discovery ,X ray astronomy has made huge steps with a number of telescopes which try to find answers about the nature, formation and evollution X-ray Binary systems.

1.1 Definition and Classification of X-ray Binaries

An X-ray binary system (XRB) is composed by a compact object, neutron star (NS) or black hole (BH), and a companion star. The compact object, which is called the accretor, orbits around the companion star,which is called the donor star, and accretes matter from it. Because of the enormous gravitational field of the compact object the matter from the donor star is accelerated to extremely high velocities. In this process the potential energy of the infalling matter is converted to the kinetic energy and eventually to heat (10^7 K to 10^8 K) radiation which lies in the region of X-rays in the electromagnetic spectrum. Thus, on these systems the accretor dominates on X-rays and the donor dominates on the optical spectrum. Given the nature of the compact objects we may have Black-Hole (BH), Neutron Star (NS) and White Dwarf (DW) systems.

An alternative way to classify the various types of XRBs is based on the mass of the companion star. The Low-Mass X-Ray Binary (LMXB) systems have a companion star with a typical mass of $1M_{\odot}$ or less with a spectral type later than B. On the other hand the High-Mass X-Ray Binary (HMXB) systems have a companion star with a typical mass of $> 10M_{\odot}$ and the star belongs to an early spectral type OB. Depending on the way the matter is accreted on the compact object the HMXBs are divided in two subcategories: Be/X-Ray Binaries(BeXRBs) and supergiant X-Ray Binaries (sgXRBs). If the material is accreted onto the compact object by strong stellar winds we have a sgXRB. On the other hand if we have accretion by a circumstellar disk we have a BeXRB. In our galaxy 300 high energy binary systems are known: 187 LMXBs and 114 HMXBs(4).

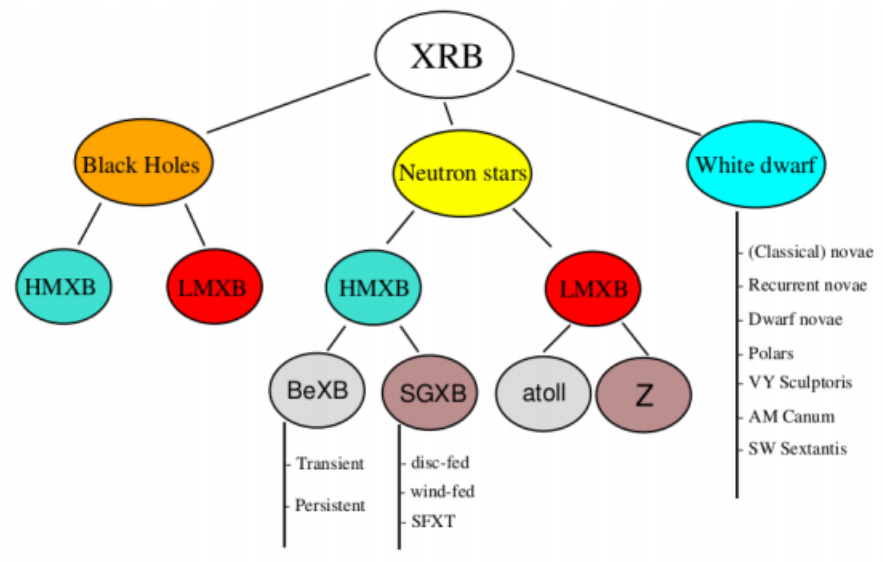

Figure 1: Classification of X-ray binaries (6)

1.2 High-mass X-ray Binaries: Formation and Evolution

Below in Figure 2 there is a schematic representation of the formation of a HMXB. Depending on the available material and the geometry of the orbit of the systems, their X-Ray emission can be either persistent or variable in timescales of days up to several months. Their tyical luminosity ranges are between $\sim 10^{34}$ (for low-activity systems) up to $10^{38} ergs^{-1}$ (for outburtsing systems)(8). Before the formation of a HMXBs we have a binary system with stars at Zero Age Main Sequence-ZAMS) with masses over $8M_{\odot}$. The primary star which is the most massive will evolve fast and in a few Myrs will fill its Roche-lobe, transfer most of its mass to its companion and finally will explode as a supernova. Under the condition that the binary system will survive from the explosion, the stellar remnant will remain in a wider and more eccentric orbit than the initial one, because of the gravitational potential of the system. After that the roles reverse and the secondary star in now the most massive. Depending on the nature of this star the accretion of matter to compact object can be either through stellar wind or an equatorial disk. At this point the system enters in HMXB stage. But, these systems are dynamic so the evolution does not stop at HMXBs. As the binary evolves the orbital period gradually becomes shorter because of the angular momentum loss. When the orbit shrinks to such a degree that the compact object is at the vicinity of the companion's envelope the binary enters the common envelope phase. This period is a very short-lived phase of a few $\sim 10^3$ yrs and the compact object spirals in and its orbital energy is deposited to the envelope. If the binary system has enough energy to eject the envelope before the compact object merges with the stellar core, the helium core of the secondary component of the binary evolves fast and leads to a second supernova explosion. The remnants of the binary are now two neutron stars and leads to potential gravitational wave system. (10).

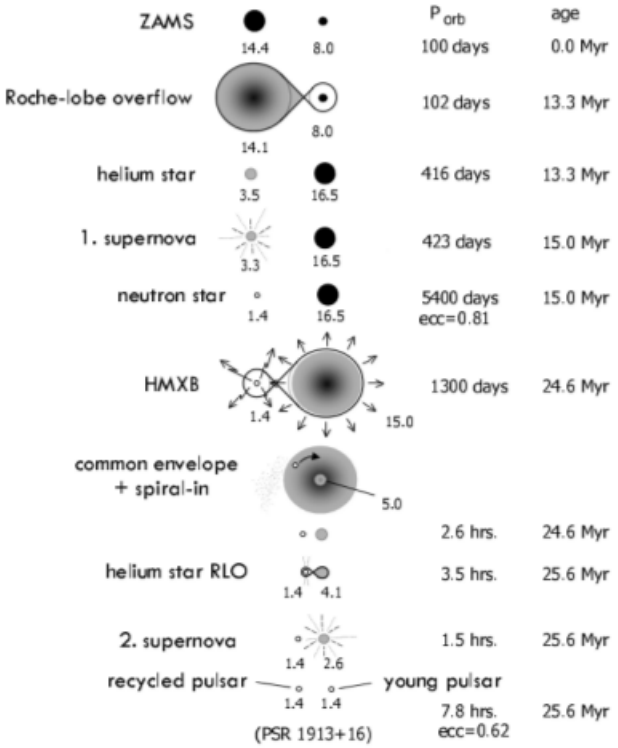

Figure 2: Schematic representation of the formation and evolution of a HMXB.The orbital period and the time evolution are also presented inline with the various evolution stages up to and after the HMXB phase. (7)

1.2.1 Be/X-ray Binaries

A Be/X-ray binary system is consists of a non-supergiant B star (with luminosity class III-V) and a neutron star. The main characteristic is that the donor's star spectrum has, or had at some time, one or more Balmer lines in emission. That explains the symbol "e"(from the word "emission") after the spectral type. In this definition are included also stars with spectral type late O of similar luminosity class that present emission lines.Below in Figure 3 we present a shematic figure of a BeXRB system. Actually, there is no physical reason to exclude black holes but based on population synthesis modes and evolution models is estimated that the ratio of BeXRBs with neutron stars to those with black holes is $\sim$ 30-50, and if applied to the number of known Galactic BeXRBs results to $\sim$ 0-2 systems with black holes. Generaly the ratio is a natural outcome of (i) the stellar initial mass function that produces more neutron stars than black holes and (ii) common envelope evolution (i.e. a major mechanism involved in the formation of interacting binaries) that naturally selects progenitors of Be X-ray binaries with neutron stars (binaries with comparable mass components have more likely survival probabilities) over ones with black holes (which are much more likely to be common envelope mergers).(11)

Material is expelled from the star due to its very high (close to the critical limit) rotational velocity (8). Then this mass is accumulated in a form of an equatorial decretion disk. When the NS passes from the periastron (the closest to the star point of its orbit) it attracts matter

from the disk and creates an accretion disk. This is the phase we have intense X-ray emission. Gradually, this emission decreases as the NS travells farther in its orbit and depending on the eccentricity and available material the emission can become undetected.So the most BeXRBs are transient systems.

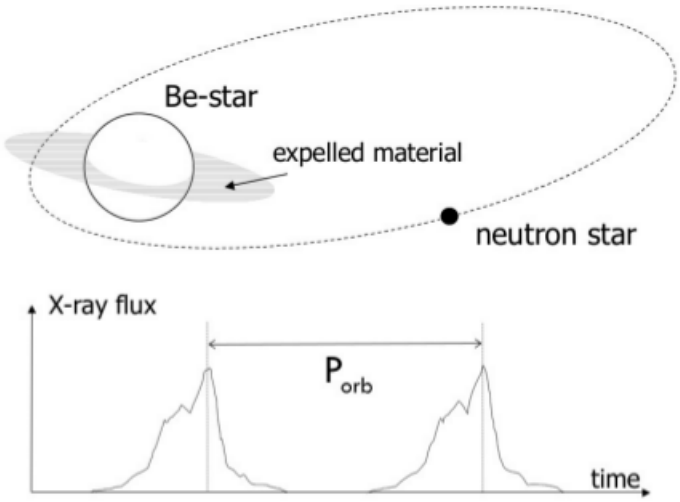

Figure 3: Schematic representation of a BeXRB. As the NS passes close to the star, it accumulates material from the disk of the donor Be-star and enters an outburst event of Type I. The X-ray flux decreases (to a non-outbursting, often non-detectable phase) as the neutron star orbits away from the donor, and its flux raises again after one orbit when it approaches the periastron again. (7)

BeXRBs are divided in two subcategories depending on outbursting activity.

- *Type I outbursts*: Are regular and periodic each time the NS crosses the decretion disk at periastron. Their duration lasts a few days and their outburst luminosities are in the range of $10^{36} - 10^{37} ergs^{-1}$ (8).
- *Type II outbursts*: On the other side, in this category belong giant outbursts which are aperiodic, with a dramatic expansion of the NS(9).The flux in these cases is highly increased($10^3 - 10^4$ times the non-outbursting state(7)) and makes these systems the brightest X-ray sources among the sky.

1.2.2 Optical/IR properties of BeXRBs

There are two main observational characteristics of Be stars, the emission spectral lines and an excess of IR emission. Both are coming from the optical counterpart because of its domination on the optical and the IR part of the electromagnetic spectrum and are result of the free-free and free-bound emission from the disk(9). More specifically, as the disk is irradiated by the star, it is ionized and the recombination of free electrons results to the emission of Balmer lines in the optical part. The most significant line is the H_α at 6563Åbut others lines are possible also. The study of H_α line (intensity and profile) provides informations about the Be disk. (size,velocity ,density)(6). More specifically the study of "violet-to-red" (V/R) variations of the H_α which is an observational phenomenon can provide us with vary usefool informations for the nature of the disk.V/R variations are phenomena caused by the global m = 1 oscillations and reflect the movement of a denser region in the equatorial disk (12). The IR emission is continuum due to recombination of the electrons with the ionized atoms(7).

1.2.3 Supergiant X-ray Binaries

These systems host a NS or a BH in orbit around an early type supergiant OB donor star with luminosity class I-II. Depending on the mass transfer mechanism they are seperated in two distinct groups. Roche lobe overflow (RLOF) and wind-fed systems. The first category constitutes the classical bright sgHMXBs with accreted matter via inner Lagrangian point to the accretion disc. So,this process causes a high X-ray luminosity $L_x \sim 10^{38} ergs^{-1}$ (9). The wind-fed sgXRBs are close systems with a low eccentricity. The donor star loses mass through a strong radial and highly supersonic stellar wind. The mass-loss rates are between $10^{-8} - 10^{-6} M_\odot$ and the X-ray luminosity is much lower $\sim 10^{35} - 10^{36} ergs^{-1}$(8).The compact objects in the sgXRBs are found generally in low eccentricity close orbits ($P_{orb} \sim 3 - 40 days$) so the accretion of matter is continous and the sgXRBs are persistent systems.

1.3 Low-mass X-ray Binaries: Definition, Formation and Evolution

LMXBs are systems in which the companion star has a tyical mass of $1 M_\odot$ or less with a spectral type much later than B. Below in the Figure 4 there is a schematic representation of the formation of a LMXB. In the case of LMXBs the small and low mass companion star fills and overflows its Roche lobe. Therefore accretion of matter always occurs through the formation of an accretion disc. In this subcategory of XRBs the initial binary system is composed by a massive primary star and a low-mass secondary star.The most massive star evolves quickly(within a few Myrs) passing from Roche-lobe overflow and common envelope phases, and ends again in a supernova explosion.This time depends on the evolution time of the low-mass star, as a few Gyr are needed before the orbit of the system shrinks, the secondary fills its Roche-lobe, and their separation becomes smaller.Thus,the LMXBs characterize a rather older stellar population, contrary to the HMXB population.(7). Below there is a schematic representation of the formation of a LMXB.

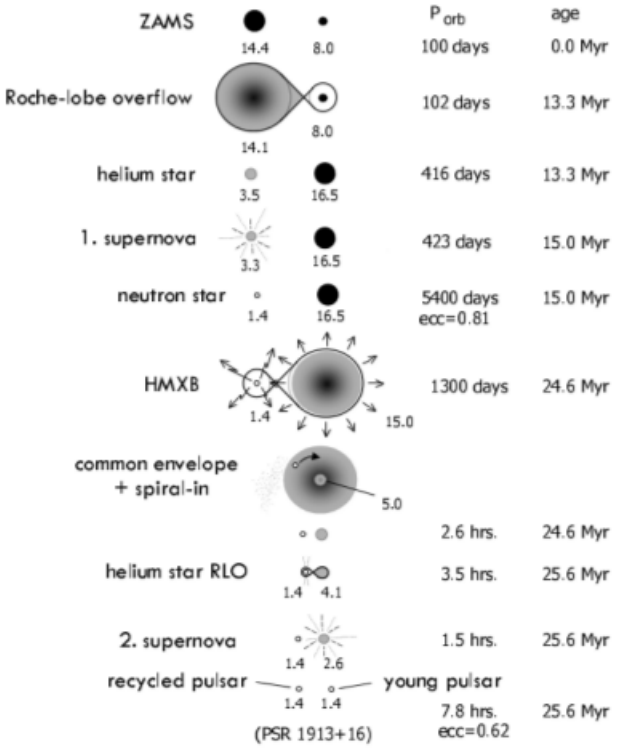

Figure 4: Schematic representation of the formation and evolution of a LMXB.The orbital period and age are also presented inline with the various evolution stages up to the LMXB phase.(7)

1.4 The Galactic HMXB distribution

The distribution of the HMXBs in our galaxy is not at all random. HMXBs can be found along the galactic plane and the spirals arms indicating an association with star-forming regions and the younger stellar population. Because of the short time which need the HMXBs to form they do not have enough time to travel very far from their forming regions (7). On the other hand LMXBs are distributed around the galactic centre and also in regions further away than the centre. All the above are presented in below figures. In Figure 4 we show the spatial distribution of HMXBs and LMXBs in our Galaxy. In Figure 5 we show the asocciation between star-forming areas and HMXBs.

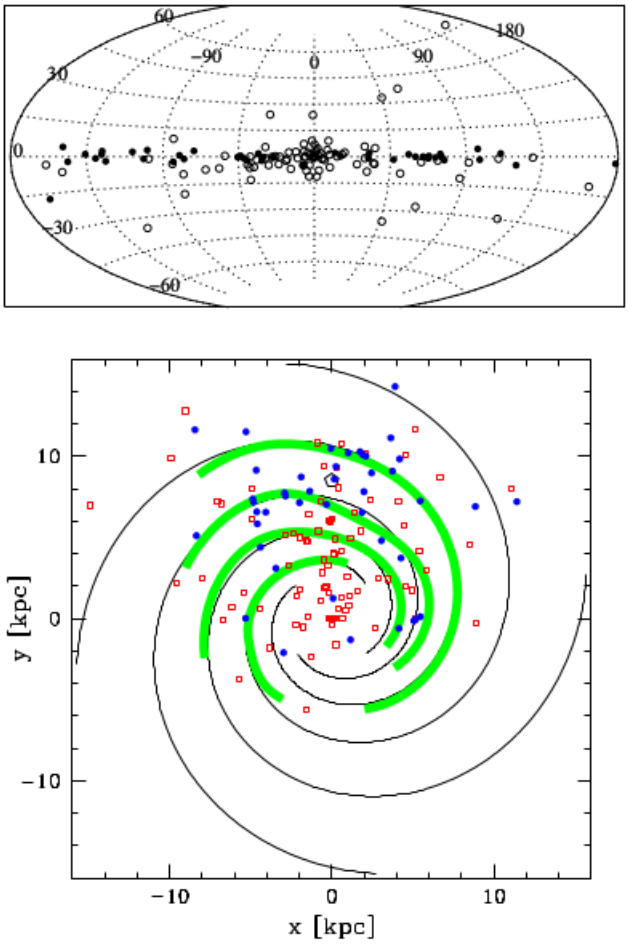

Figure 5: Top panel: The distribution of LMXBs (86, open circles) and HMXBs (52 filled circles) in the Galaxy, representing the older stellar population (around the Galactic center) and the younger stellar population (along the Galactic plane), respectively. Bottom panel:The same distributions (LMXBs represented as open squares, and HMXBs as filled circles) as seen from a face-on view of the Galaxy. (7)

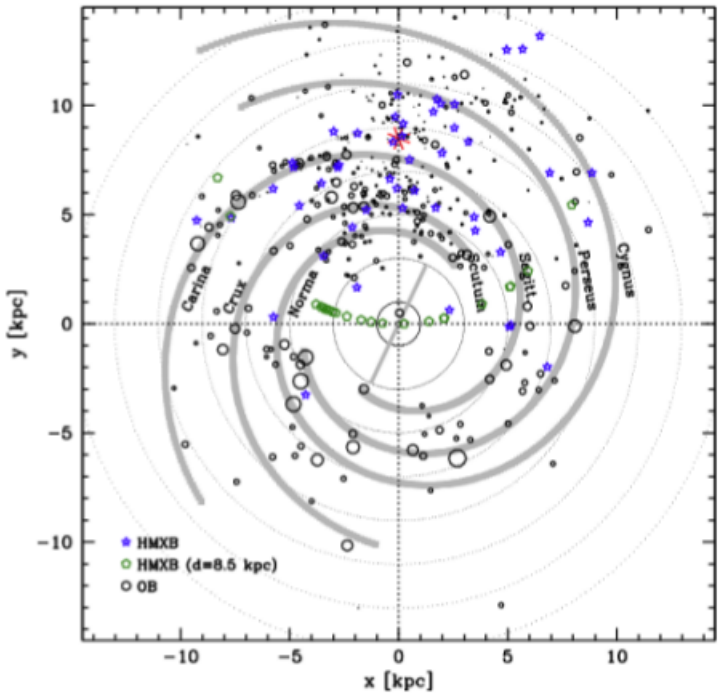

Figure 6: The distribution of Galactic HMXBs (blue stars) and star-forming regions (black circles, with sizes proportional to their star-forming rate) overplotted on a face-on model of the Galaxy.A number of sources (green pentagons) have unknown distances and they are presented at a distance of 8.5 kpc. The red star (located at x=0, y=8.5) is the position of the Sun. (7)

1.5 HMXBs in Maggelanic Clouds

The study of HMXBs in our galaxy is not an easy work. Two main problems affect the observations of HMXBs: the extinction and the distance uncertainties. Mainly in far HMXBs the extinction hampers the estimation of the actual population and their luminosities are not accurately determined because of the distance. Thus, in order to study and understand the nature of HMXBs we have to turn our telescopes in other galaxies. The best choice is to observe galaxies which are close enough to our own Galaxy and they are not affected from the above problems.

The Small Magellanic Cloud (SMC) and the Large Magellanic Cloud (LMC) are two neighboring galaxies visible on the Southern Celestial Hemisphere and they are an excellent laboratory for HMXBs. The SMC (RA:00 h 52m 44.8s, Dec:$-72°49'43$") ,which is located in a distance $d = 60.6kpc$(14), has been extensively studied in X-rays. It has 120 HMXBs of which 64 are classified as X-ray pulsars. Out of these systems only one is a sgXRB, source SMC X-1. On the other hand the LMC has receive much less attention. LMC (RA:10 h 12m 45.3s, Dec:$-45°17'50$") is a dwarf irregular galaxy in a distance $50.0kpc(\Omega)$ and it is our nearest star-forming galaxy. It has an extended circular shape with a prominent off-center bar, a nucleus and irregular arms (5). A recent census for the LMC icludes only 40 HMXBs , of which only 23 have been confirmed (5). Contrary to a comprehensive samle of the SMC , the LMC has so few confirmed HMXBs and thus is difficult to make comparisons with population synthesis and Star-formation studies. An other reason which supports a more extensive study of the LMC is its sub-solar metalllicity.

Nowadays is it accepted that metallicity is one of the the three main factors that determines the formation rate of young XRBs. There is an indication that low metallicity is asociated with higher formation efficiency of HMXBs and higher luminosity. The LMC ($1/2.5Z_{\odot}$) bridges the gap between the SMC ($1/5Z_{\odot}$) and the Galaxy. Thus, one understands that is a need to study more carefully the LMC in order to collect as much information as possible to have a more clear view of the nature, formation evolution of HMXBs in different galaxies.

1.6 Aims of the project

The main goal of this project is to make an effort to increase the sample of confirmed HMXBs in the LMC and investigate the nature of optical counterparts of 15 HMXBs candidates. In order to do that we analyzed the spectrum of each counterpart and we obtained its spectral type. After that we examined the H_{α} spectral region in order to find the line in emission, which is a strong indication of a Be star. More specific the purpose of the project is :

- To confirm or not the candidates HMXBs and increase the number of the known HMXBs in the LMC.
- To study how the spectral type distribution changes with the new additions and how does it compare with the Galactic and SMC distributions.
- To investigate how many of the confirmed HMXBs are Be/X-ray Binaries systems with emission.
- To investigate how many of them have an early type spectrum but not in emission.

2 Sample

2.1 Candidates Selection

For this work, the sample which used is derived by the list of candidate optical counterparts to HMXBs as presented in the paper of Antoniou Zezas(2016) (5). The exctraction of the X-ray sources is obtained from XMM surveys targeting the LMC, with sensitivity limit of X-ray Luminosity of $\sim 10^{33} erg/s$.Then, this list is cross-correlated with optical catalogs to identify optical counterparts. For the current work we mainly work with the OGLE-III catalog (complete down to V $\sim$ 21 mag). To properly select the optimal candidates we select those which are located within the locus of OB stars in the color-diagram and those with Ha emission, with a chance coincidence probability of $\sim 21 \pm 10\%$.So, we do not except a large number of spurious matches in our sample. Finally we are left with 23 candidate HMXBS, 15 of which are previously unclassified.

3 Observations

3.1 SOAR Telescope and Instruments

For our project the observations were acquired during three nights of service time (on Dec 10,11 and 12, 2017) at the Southern Astrophysical Research Telescope (1).The SOAR is a 4.1 meter aperture telescope which is located on Cerro Pachón - IV Región - Chile, at 2.700 meters above sea level. It can operate from UV-optical to near infrared and features fast slewing and a suite of optical and infrared instruments mounted and ready for use.

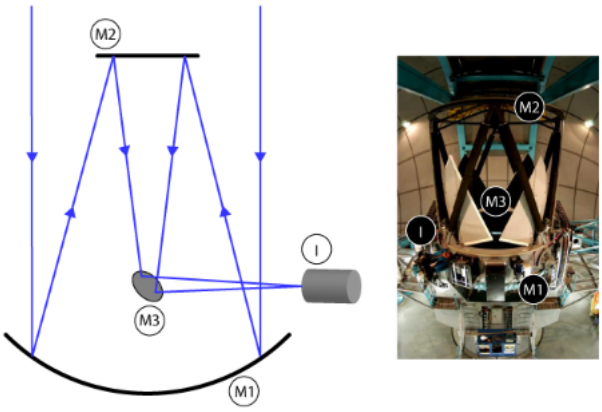

Figure 7: Telescope image(1).The light first reflects at the primary mirror M1, then at mirror M2, after at mirror M3 and finally it is concentrated at the detector I.

In order to obtain sperctra from our sources we used the Goodman High Throughput Spectograph (GHTS). The GTHS is an imaging spectrograph, capable of producing excellent image quality across a 7.2 arcmin field-of-view (fov) and the the plate scale is 0.15 arcsec/pixel.

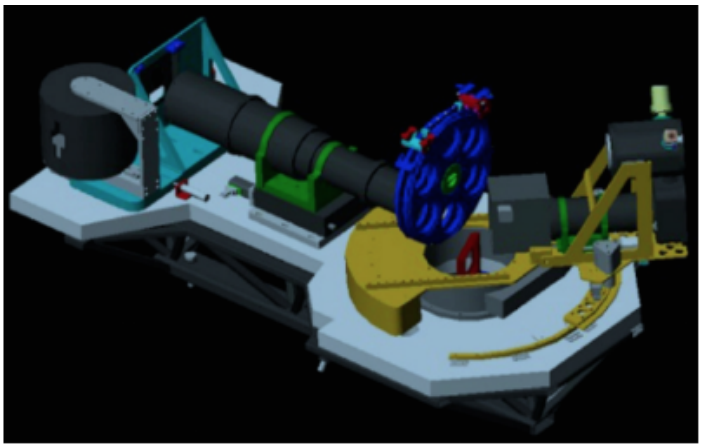

Figure 8: Shcematic representation of Goodman spectograph(1)

In spectroscopic mode the Goodman spectograph can obtain long-slit and multi-slit spectra (over a fov of 3.0x5.0 arcmins). The Goodman Spectograph operated from $320 - 900nm$ and has scale $0.15 arcsec/pixel$. The Blue Camera is optimized for the UV and the Red Camera for wavelengths larger than 400 nm .

For our scientific purpose we used the long-slit mode of the spectograph, with 1" slit width. We opted for the 600 l/mm grating to obtain the 4037-6695$\mathring{A}$ range.Also we used filter GG-385.In addition a 2x1 binning (2 in the spatial, 1 in the spectral direction) was used, in order to gain resolution.Consequently the dispersion of our observations was 0.64 A/pixel and the resolution was 3.74 $\mathring{A}$. During the observation we used the Red Camera at 344 kHz Read rate, provideing a readnoise of 3.89 and a gain of 1.48 e^-/ADU.

3.2 Table of Observations

In Table 1 we present a summary of the sources which we analyzed in this work. In column 1 we present the name of the X-Ray source and in column 2 the identity of the HMXB. In columns 3,4 we show the coordinates in the sky and in columns 5,6 we show the magnitudes in V,I filters. In column 7 we present the Signal to Noise ratio of our spectra. In order to obtain the S/N we examined each spectrum in a specific spectal range between 5000-6000 Åbecause in this way we can avoid the noise. We count the S/N in this range three times and we calculated a mean S/N value which is presented in the table. In column 8 we show the number of exposures and the exposure time for each spectrum. Finally in column 9 we present the date of the observational night.

Table 1: **Table of observations**

X-Ray source	**HMXB ID**	**R.A.(J2000)** (hh mm ss.ss)	**Dec.(J2000)** (dd mm ss.ss)	**V** (mag)	**I** (mag)	**S/N**	**Exposure** s	**Observ. night** Date
(1)	(2)	(3)	(4)	(5)	(6)	(7)	(8)	(9)
RX J0524.2-6620	16	05 24 11.83	-66 20 50.90	14.867	14.866	31	1x300,1x360	10/12/2107
XMMU J050755.4-682505	9	05 07 55.49	-68 25 04.80	14.945	14.894	14	2x360	10/12/2017
RX J0523.2-7004	15C	05 23 16.94	-70 04 00.00	15.025	14.402	25	1x900	10/12/2017
RX J0457.2-6612	4	04 57 15.39	-66 12 22.70	15.63	15.459	23	1x900	10/12/2017
Swift J0549.7-6812	B	05 50 06.49	-68 14 55.80	15.028	15.003	17	1x900	10/12/2017
RX J0507.6-6847(?)	8	05 07 38.18	-68 47 47.80	16.26	16.448	15	5x1200	10/12/2017
XMMU J053118.2-660730	26	05 31 18.66	-66 07 31.60	16.873	-	17	3x1200	10/12/2017
RX J0512.6-6717	10	05 12 41.33	-67 17 23.40	16.187	16.394	25	2x1200	10/12/2017
RX J0529.4-6952	19B	05 29 24.93	-69 52 19.70	16.508	16.608	20	2x1200	10/12/2017
RX J0529.4-6952	19A	05 29 24.93	-69 52 19.70	18.811	18.853	12	2x1200	10/12/2017
RX J0546.8-6851	45C	05 46 48.30	-68 50 53.30	16.887	17.165	17	2x1200	11/12/2017
RX J0546.8-6851	45B	05 46 48.30	-68 50 53.30	17.890	17.934	4	2x1200	11/12/2017
RX J0523.2-7004	15A	05 23 14.22	-70 04 15.80	15.129	14.094	16	3x900	11/12/2017
RX J0523.2-7004	15B	05 23 14.22	-70 04 15.80	16.965	17.151	12	3x900	11/12/2017
RX J0530.7 -6606	21	05:30:11.37	-65:51:23.5	14.877	14.691	21	2x300	11/12/2017
XMMU J052947.4-655639	20	05 29 47.82	-65 56 43.40	14.594	14.741	18	2x300	11/12/2017
RX J0456.9-6824	3	04 56 55.07	-68 24 27.60	18.283	18.287	12	4x1500	11/12/2017
RX J0530.7-6606	23A	05 30 48.60	-66 06 35.50	18.082	-	12	4x1380	11/12/2017
RX J0541.4-6936	39C	05 41 20.10	-69 36 22.90	11.79	11.91	18	1x300	12/12/2017
IGR J05007-7047	5	05 00 46.08	-70 44 35.80	14.727	14.662	15	2x300	12/12/2017
XMMU J052016.0-692505	13	05 20 16.15	-69 25 05.30	14.944	14.665	17	2x300	12/12/2017
Swift J053041.9-665426	22	05 30 42.13	-66 54 30.10	15.321	15.586	11	3x300	12/12/2017
RX J0531.5-6518	27	05 31 36.81	-65 18 16.10	16.007	16.226	4	3x900	12/12/2017
RX J0527.1-7005	17A	05 27 06.99	-70 05 00.30	15.308	13.713	5	3x438	12/12/2017
RX J0541.4-6936	39B	05 41 22.93	-69 36 33.30	17.323	17.243	17	4x1380	12/12/2017
RX J0541.4-6936	39A	05 41 22.93	-69 36 33.30	18.650	18.539	7	4x1380	12/12/2017

4 Data processing and analysis

For our project we used a standard set of spectroscopic data. For all objects we obtained a number of exposures. In addition for each set of exposure we obtained also a set of comparison lamps exposures which were used for the wavelength calibration. Furthermore bias and flat-field exposures were taken in order to propery correct the raw exposures for noise due to the camera and variations due to optical path, respectively.

4.1 Initial data reduction

In this project the data were reduced using **IRAF**(2) and **PyRAF** which is a Python wrapper for the IRAF tasks. IRAF is the Image Reduction and Analysis Facility, a general porpuse software for the reduction and the analysis of astronomical data. IRAF was produced by National Optical Astronomy Observatories (**NOAO**), in Tuscon, Arizona and it is an extremely important and usefull tool for all the astronomers around the world. The procedure which we followed for the initial data reduction is described in the subsections below.

4.1.1 BIAS substraction

BIAS frames are images of zero second exposure time obtained with the camera's shutter closed. These images contain only noise due to the camera electronics and they used in order to remove the noise from the scientific images. In order to start the bias subtraction procedure we first combined all the bias frames in one master bias image by using the IRAF's `imcombine`. After that we substructed this master bias image from our raw images and flat field frames by using an IRAF's `imcombine`/*`ccdproc`*.

4.1.2 Flat field correction

Flat-field frames are images of an approximate flat light source which have been obtained with the same layout as the observational data.The flat-fielding process is used to correct the pixel to pixel variations along the detector's surface.These variations may be due to dust, dirt or the optical path. The flat field images obtained by observing a white screen on the dome. Thus, the bias subtracted images were FLAT field corrected. To do that we combined all bias substructed flat field frames, by using again the IRAF's `imcombine`, in one master flat field image.Then we devide all the raw images by using again the IRAF's `imcombine`/*`ccdproc`*.

4.1.3 Extraction of the source spectrum

The last step in the initial data reduction was to extract the final spectrum of each source. In order to do this we used the IRAF's *`apall`*.First we identified the spectrum on the 2D image and defined the extraction and the background windows.More specifically the size of the extraction window was determined by 5 pixels left and right of the center of spatial profile. Similary, the background window was determined by 25 pixels(in most cases) left and right of the center of the profile and its range was determined by 15 pixels (in most cases). In Figure 9 we present an example image of the aperture selection and background samples. Afterwards, we traced the center of spatial profile as a function of the dispersion axis. In Figure 10 we show an example image of the trace fitting window. This is a necessary step because a typical problem with spectra is that the exact center of the spatial profile shifts slightly with the position along the dispersion axis,due to the optical distortions of the optical path.Then the program calculated for each dispersion bin the total flux derived from the pixels around the center of the spatial profile

and an average sky value derived from the background sky ranges. Finally, the final spectrum of each source was obtained by substracting the average local sky value from the observed flux.

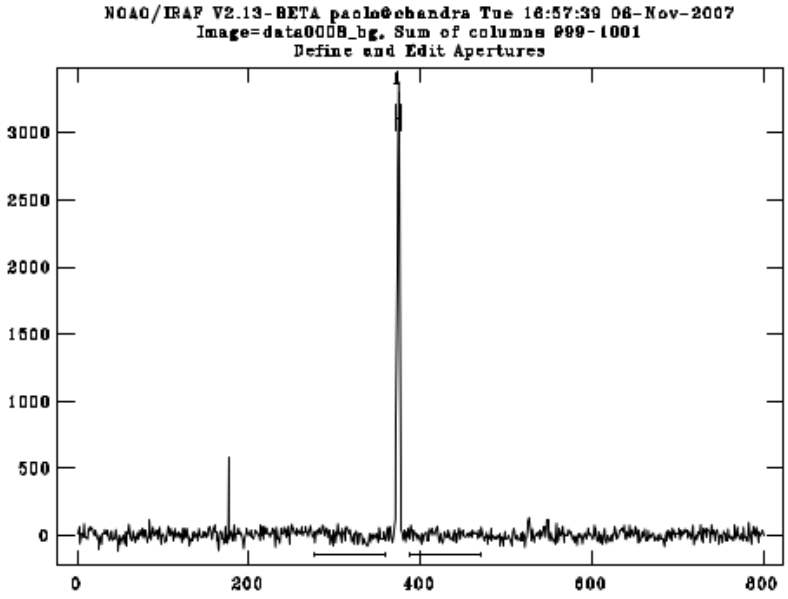

Figure 9: Aperture selection. Background samples are highlighted(13)

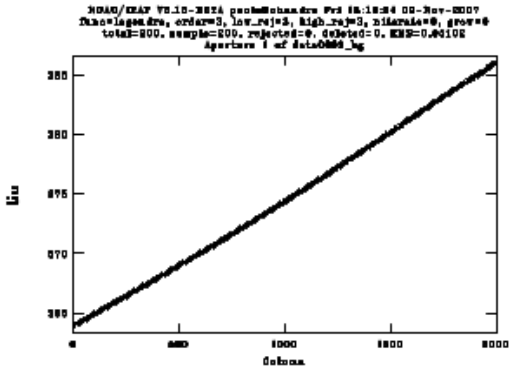

Figure 10: Trace fitting window(13)

4.1.4 Extraction of the comparison lamp spectrum

The next step was the exctraction of the comparison lamp spectrum.For our project,we used the spectrum of a HgAr Ne comparison lamp. In Figure 11 we show the spectrum of the comparison lamp. We chose this lamp because our observations were made in the wavelength range 4000-

6700 $\mathring{A}$. A number of comparison lamp exposured was taken before and after each observation. For this step we followed the same procedure as for the object spectrum.

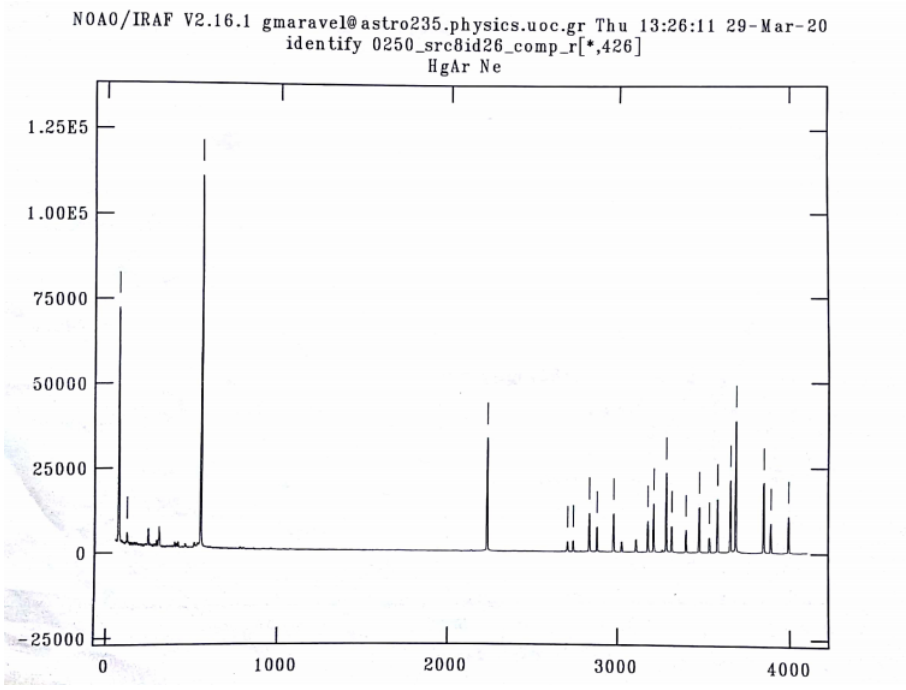

Figure 11: Spectrum of HgArNe comperison lamp

4.1.5 Wavelength calibration

Fot the wavelength calibration we used the IRAF's */identify* and the IRAF's *dispcor*.First by using *identify* we gave manually the wavelength values of some known lines of the arc lamp spectrum and then the programm automatically calculated the corresponding disppersion and indicated all lines that could be detected. We properly selected the correct lines to provide a more accurate solution. Afterwards, by using the IRAF's *dispcor* we applied the previous disppersion solution to the spectrum and finaly we exctracted object's spectrum calibrated in terms of $\mathring{A}$.

4.1.6 Combination and production of the final source spectrum

The last step of our initial data analysis was to produce the final spectrum for each source. In order to do that we combined the callibrated exposures for each source in one very final source spectrum. Thus, by combining spectra yields to a better Signal to Noise Ratio and reject cosmic rays. For this process we used the IRAF's *scombine*.

4.2 Spectral Classification criteria

After producing the final source spectra we continue with the spectral classification. For this process we use an IRAF's command which called `splot`. `Splot`, which is an interactive tool to display and analyze spectra. Our spectral classification is based on visual examination of each spectrum. In order to classify OB stars we use a combination of He_I, He_{II} and metal lines, as it is presented in Table 1. We are focused in the blue part (4000-5000 $\mathring{A}$) because this sprectral region are includes all the spectral lines which used as indicators for the classification. Also we examine the spectral region where the H_α line is located ($6540 - 6600\mathring{A}$) because its existance in emission is a strong indicator of a Be-XRB system.

Table 2: Classification criteria for B-type stars in SMC from Maravelias et al. (2015).

Line identifications	Spectral Type
HeII λ4200,HeII λ4541,HeII λ4686 present	earlier than B0
HeII λ4541 and HeII λ4686 present, HeII λ4200 weak	B0
HeII λ4200 and HeII λ4541 absent, HeII λ4686 weak	B0.5
HeII λ4686 absent, SiIV $\lambda\lambda$4088,4116 present	B1
SiIV λ4116 absent, SiIII λ4553 appear	B1.5
OII+CIII λ4640-4650 blend decreases rapidly	later than B1.5
SiIV and SiII absent, MgII λ4481< SiIII λ4553	B2
MgII λ4481 $\sim$ SiIII λ4553	B2.5
MgII λ4481> SiIII λ4553	B3
OII+CIII λ4640-4650 blend disappears,	later than B3
OII λ4415-4417, NII λ4631 disappear	
clear presence of HeI λ4471 and absence of MgII λ4481	earlier than B5
SiIII λ4553 absent, SiII $\lambda 4128 - 4132<$ HeI λ4121,	B5
HeI λ4121< SiII $\lambda 4128 - 4132<$ HeI λ4144,	B8
MgII λ4481 $\leq$ HeI λ4471	
HeI λ4471< MgII λ4481,	B9
FeII λ4233< SiII λ4128-4132	

5 Results

In this chapter we present the results of our spectra classification. In the following sections we give a small description on the spectral type we assigned to each source individually. In Figure 12-15 we present the spectra regions we are interested in for the classification and the region around H_α. We note here that between the quoted wavelengths in Table (1) and the observed features of our spectra there is a small difference due to the redshift effect. The LMC moves away from our galaxy with a velocity of 262 km/sec. Consequently the difference between the observational and laboratory wavelengths is about a factor 0.000874 or 3.67 $\mathring{A}$.

Figure 12: **Spectral regions for the blue part and H_α for the source ID:4**

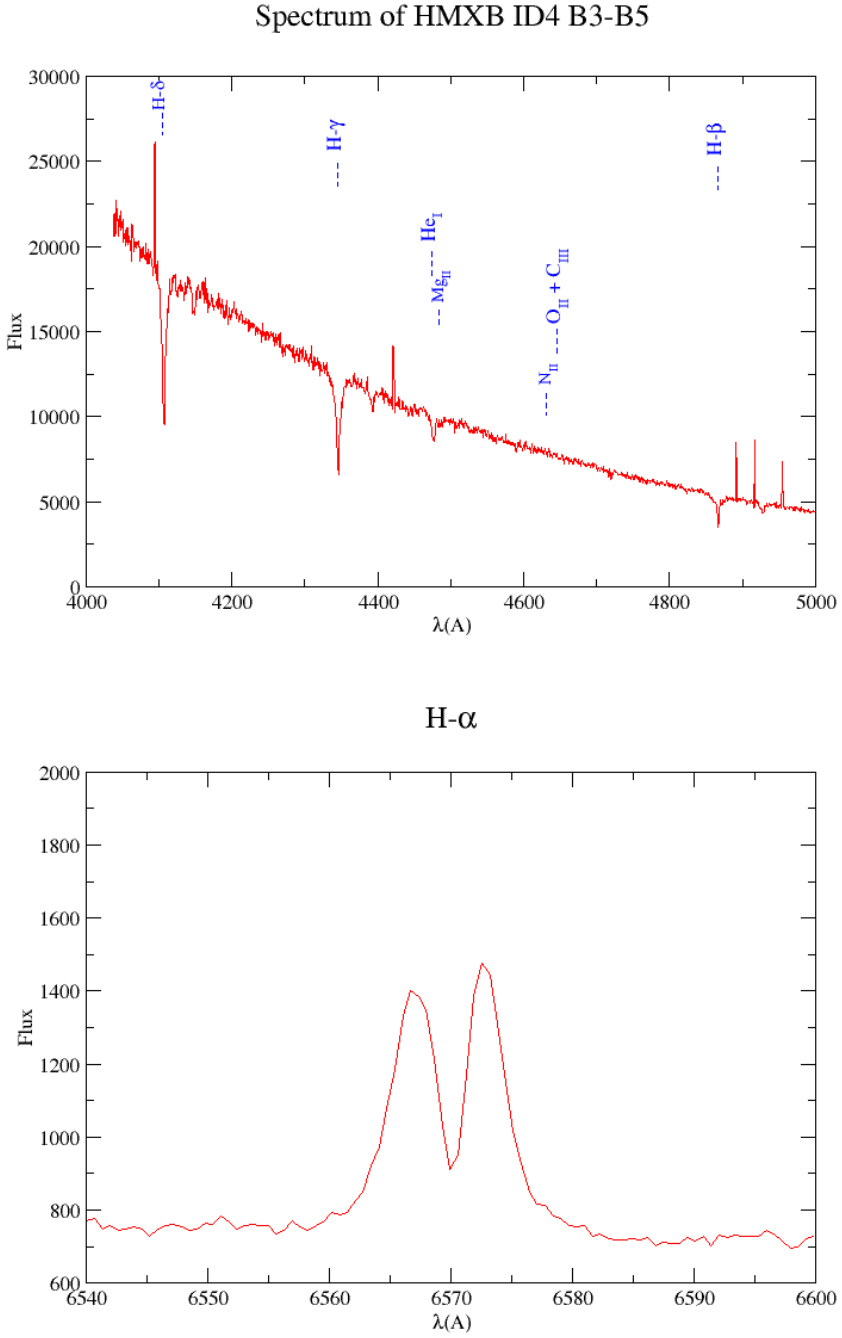

Figure 13: **Spectral regions for the blue part and H_α for the source ID:5**

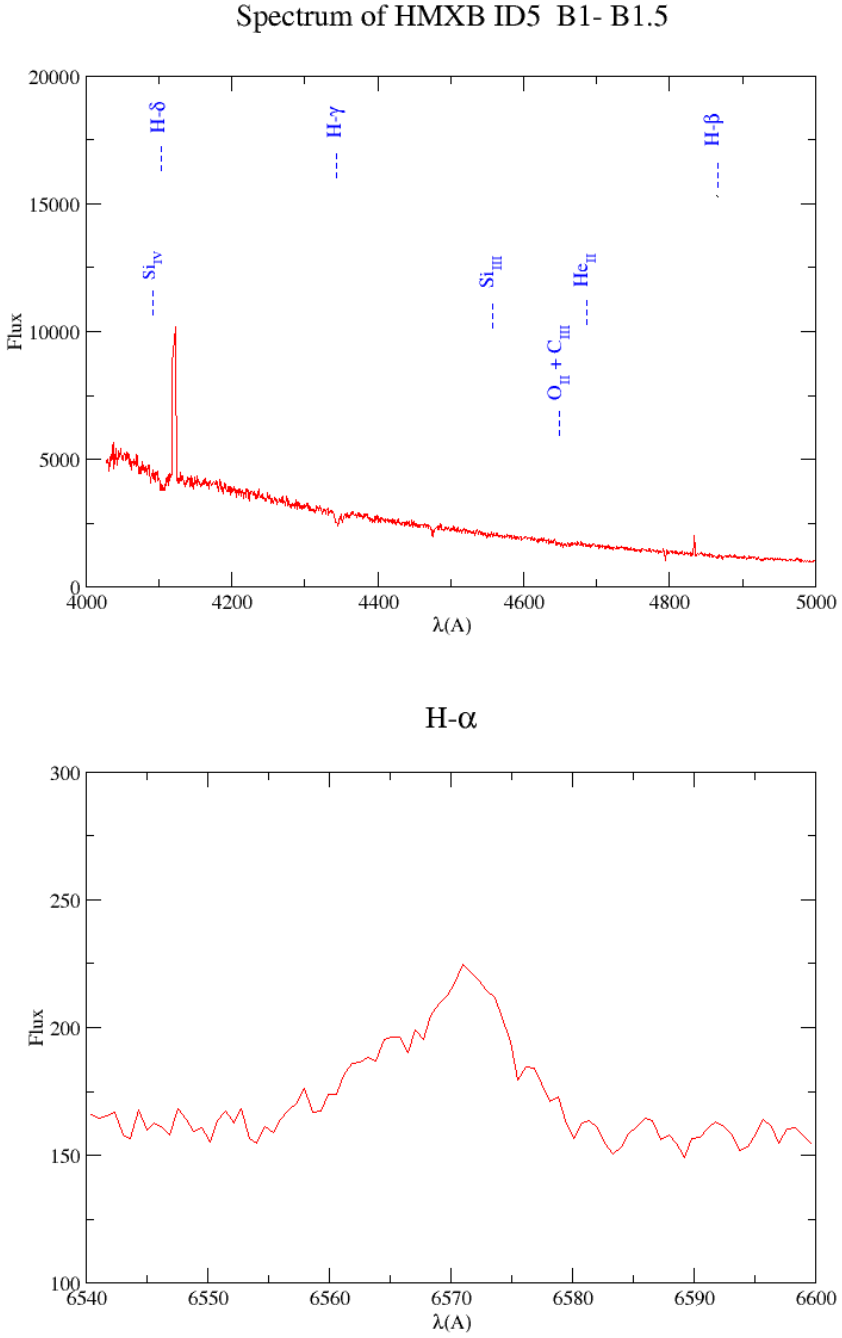

Figure 14: **Spectral regions for the blue part and H_α for the source ID:8**

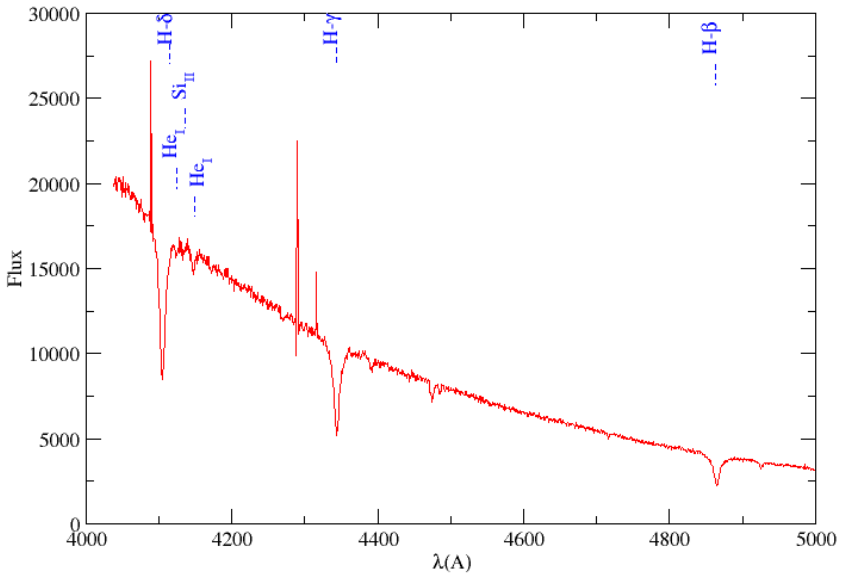

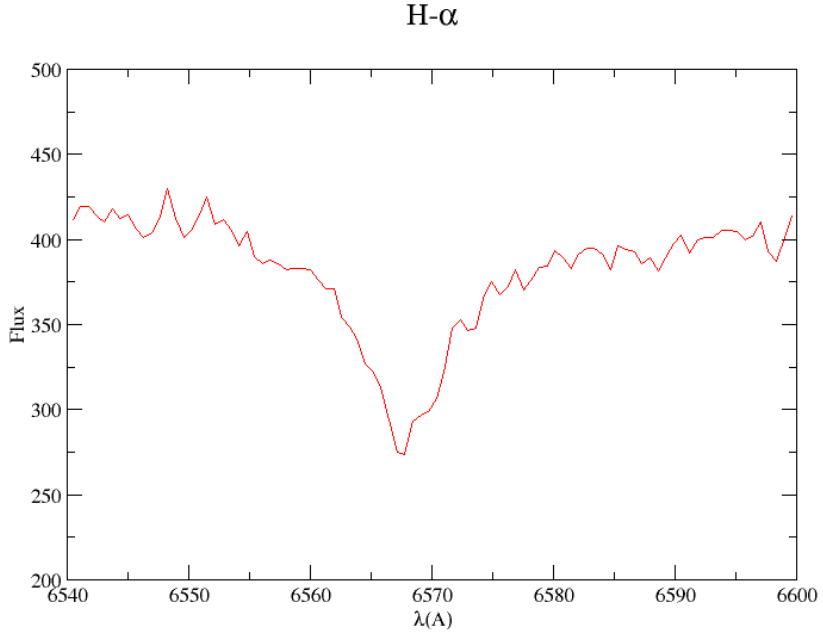

Figure 15: **Spectral regions for the blue part and H_α for the source ID:9**

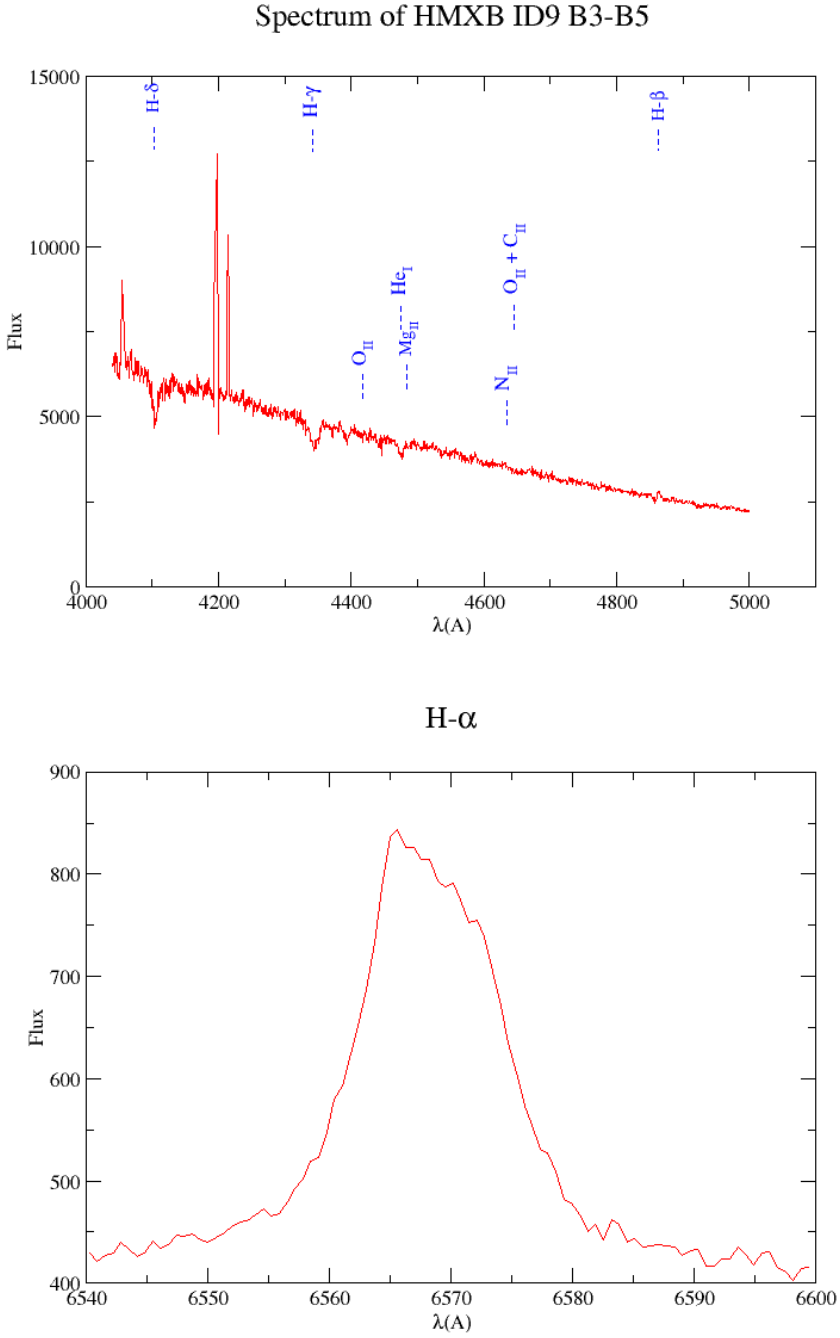

Figure 16: **Spectral regions for the blue part and H_α for the source ID:10**

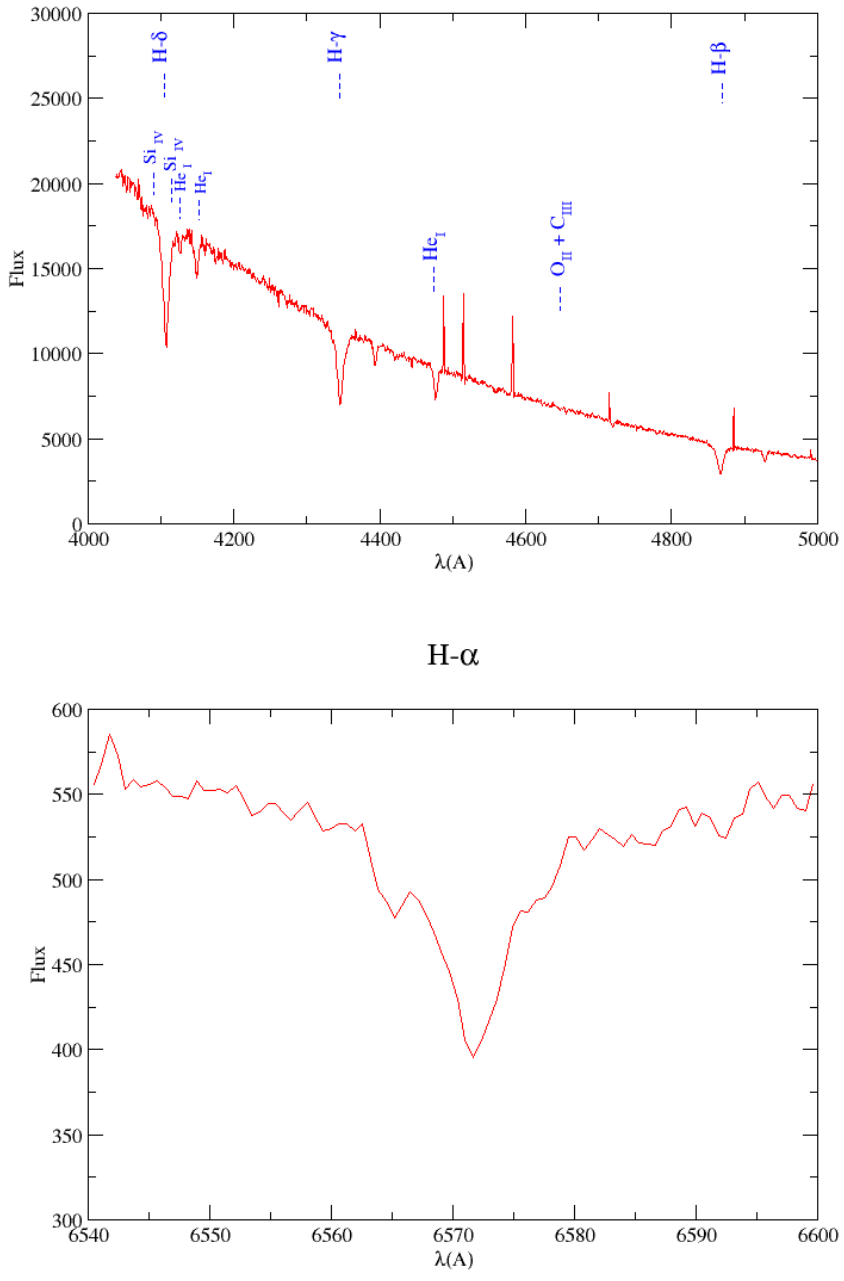

Figure 17: **Spectral regions for the blue part and H_α for the source ID:13**

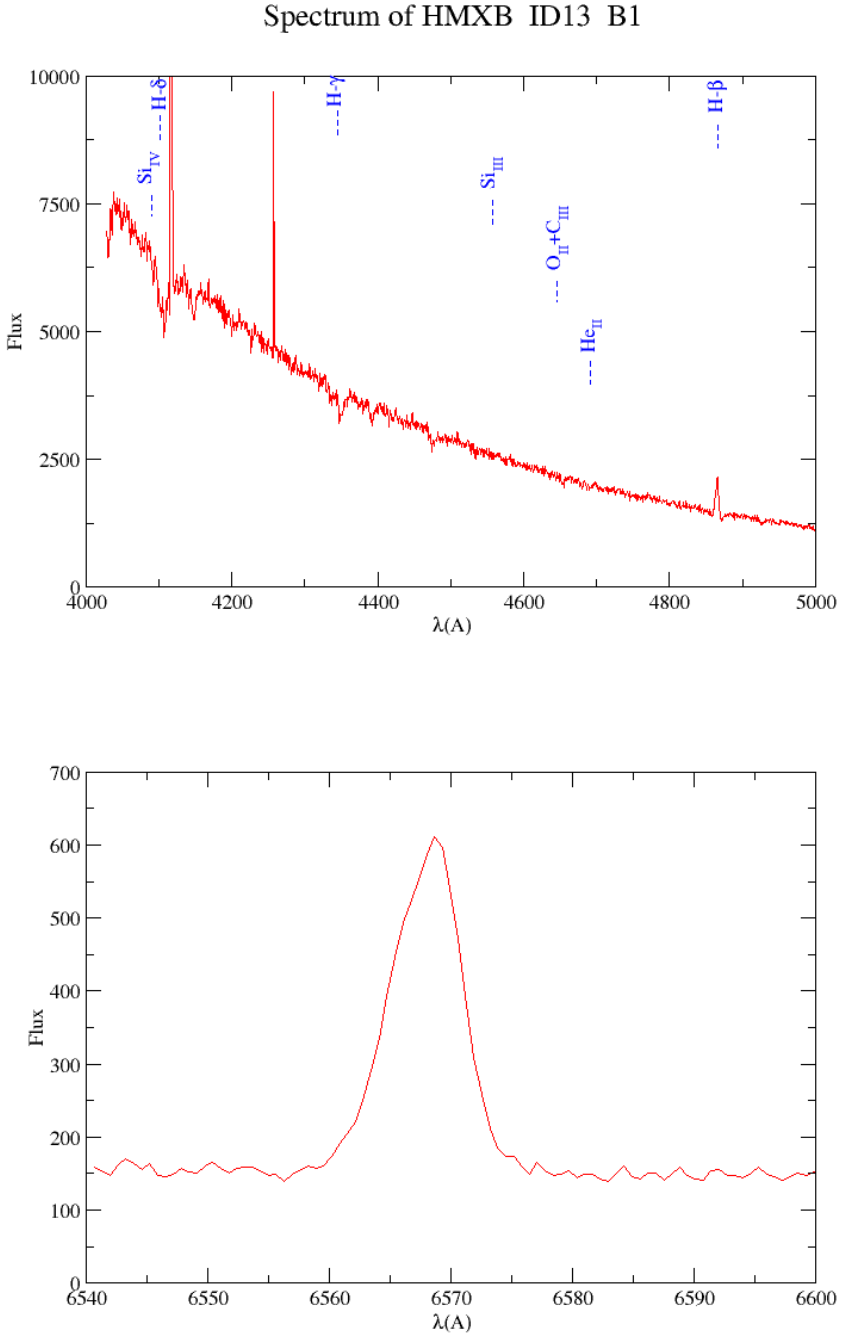

Figure 18: **Spectrum for the source ID:15A**

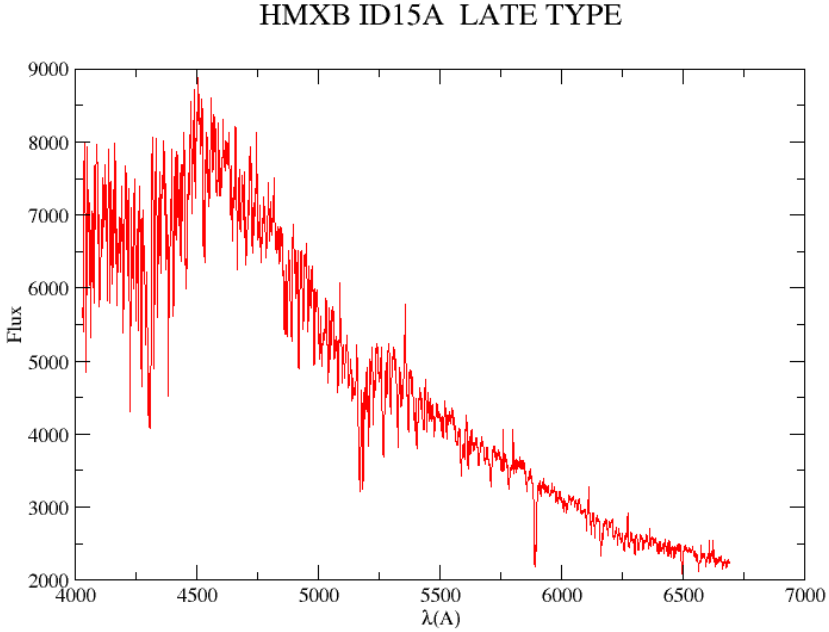

Figure 19: **Spectral regions for the blue part and H_α for the source ID:15B**

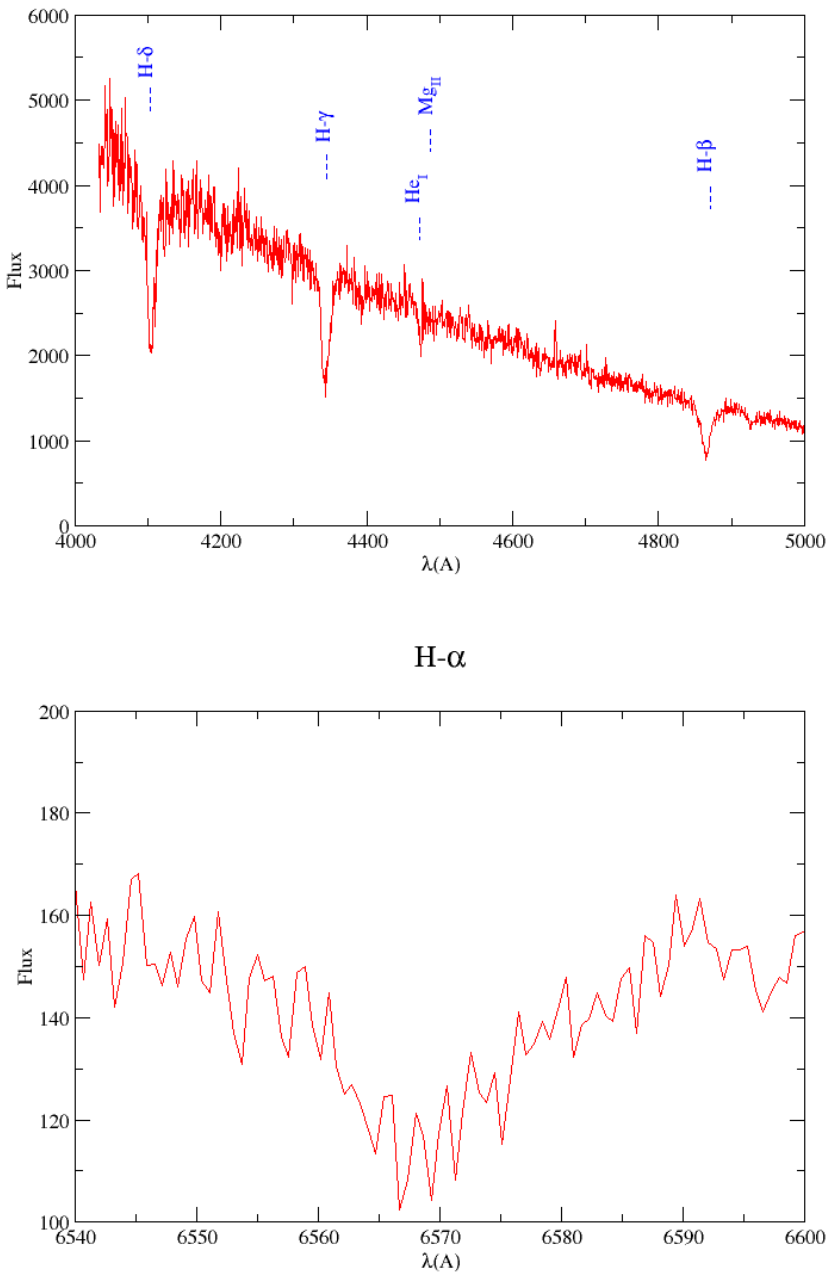

Figure 20: **Spectral regions for the blue part and H_α for the source ID:15C**

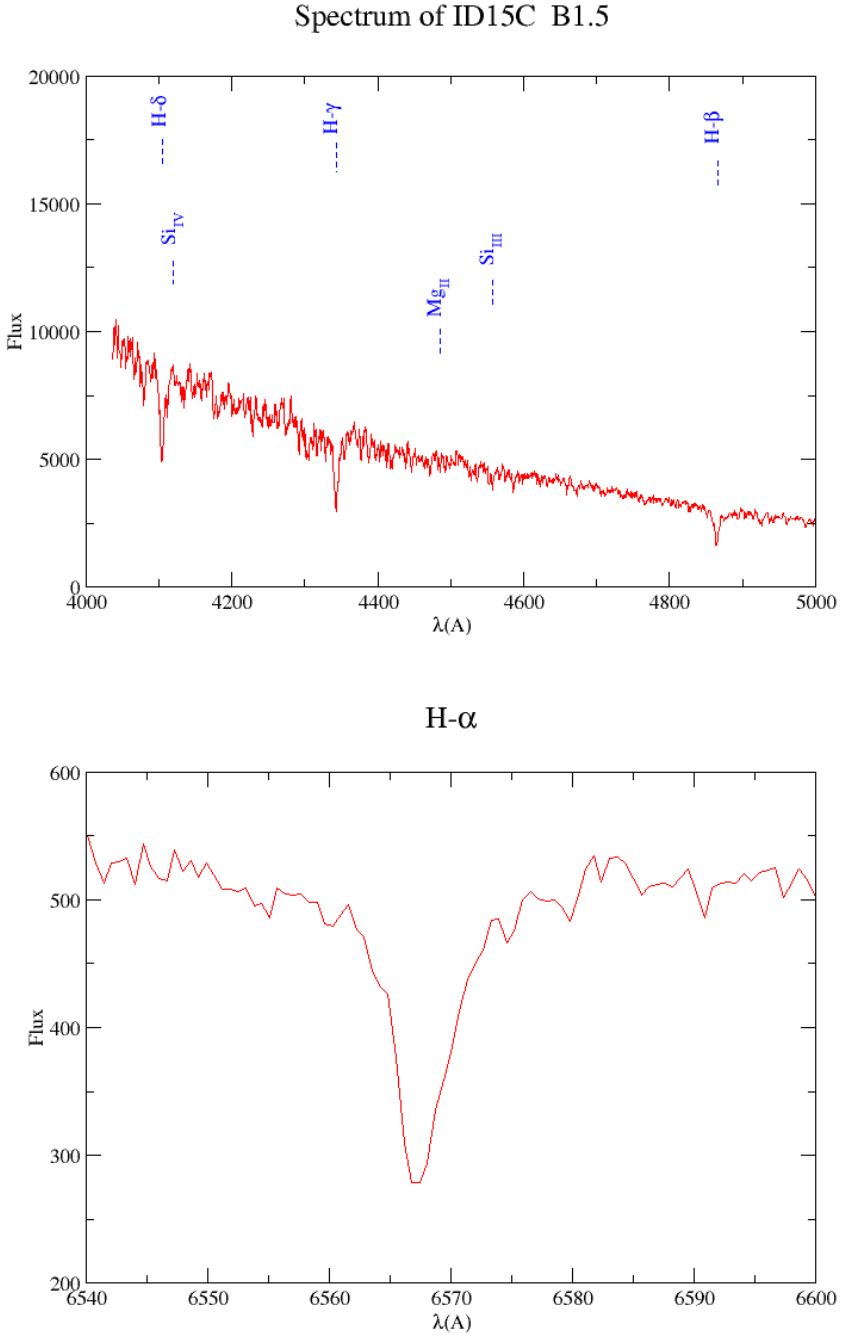

Figure 21: **Spectral regions for the blue part and H_α for the source ID:16**

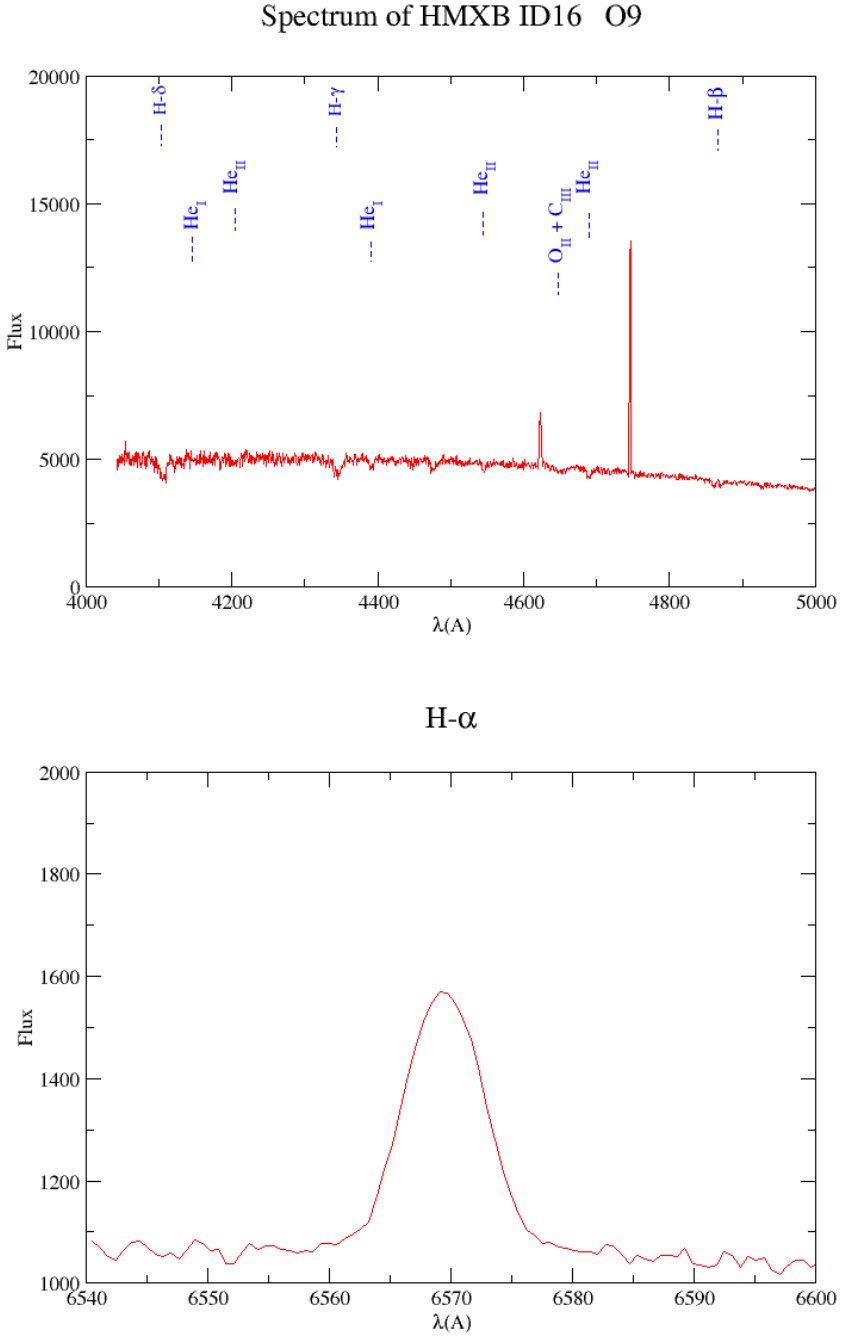

Figure 22: **Spectrum for the source ID:17A**

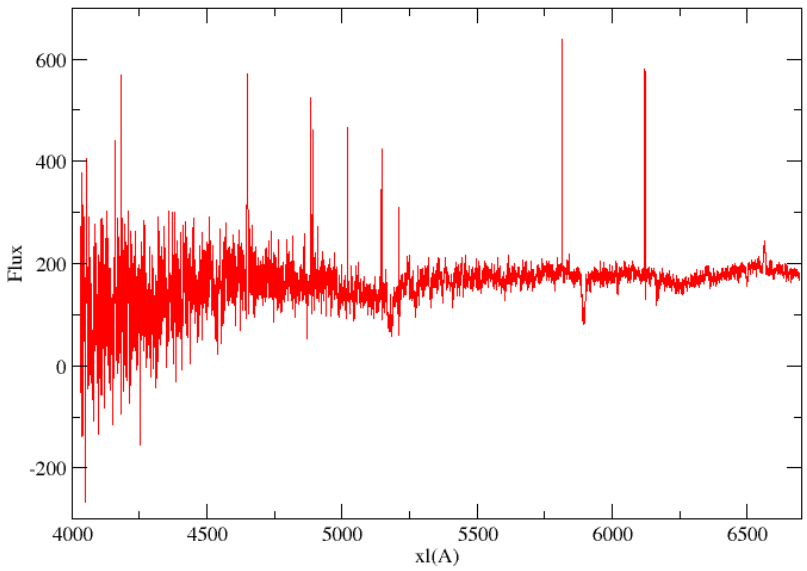

Figure 23: **Spectral regions for the blue part and H_α for the source ID:19A**

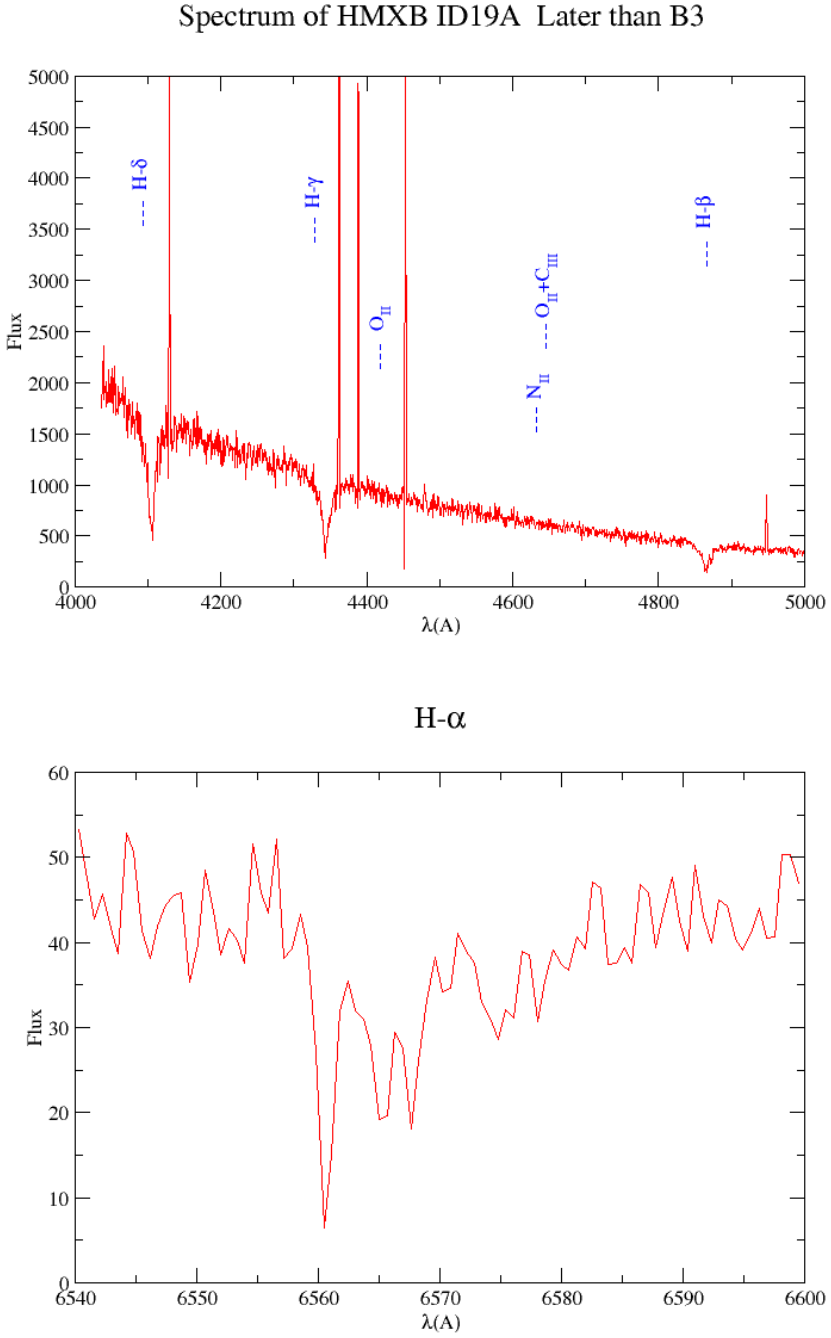

Figure 24: **Spectral regions for the blue part and H_α for the source ID:19B**

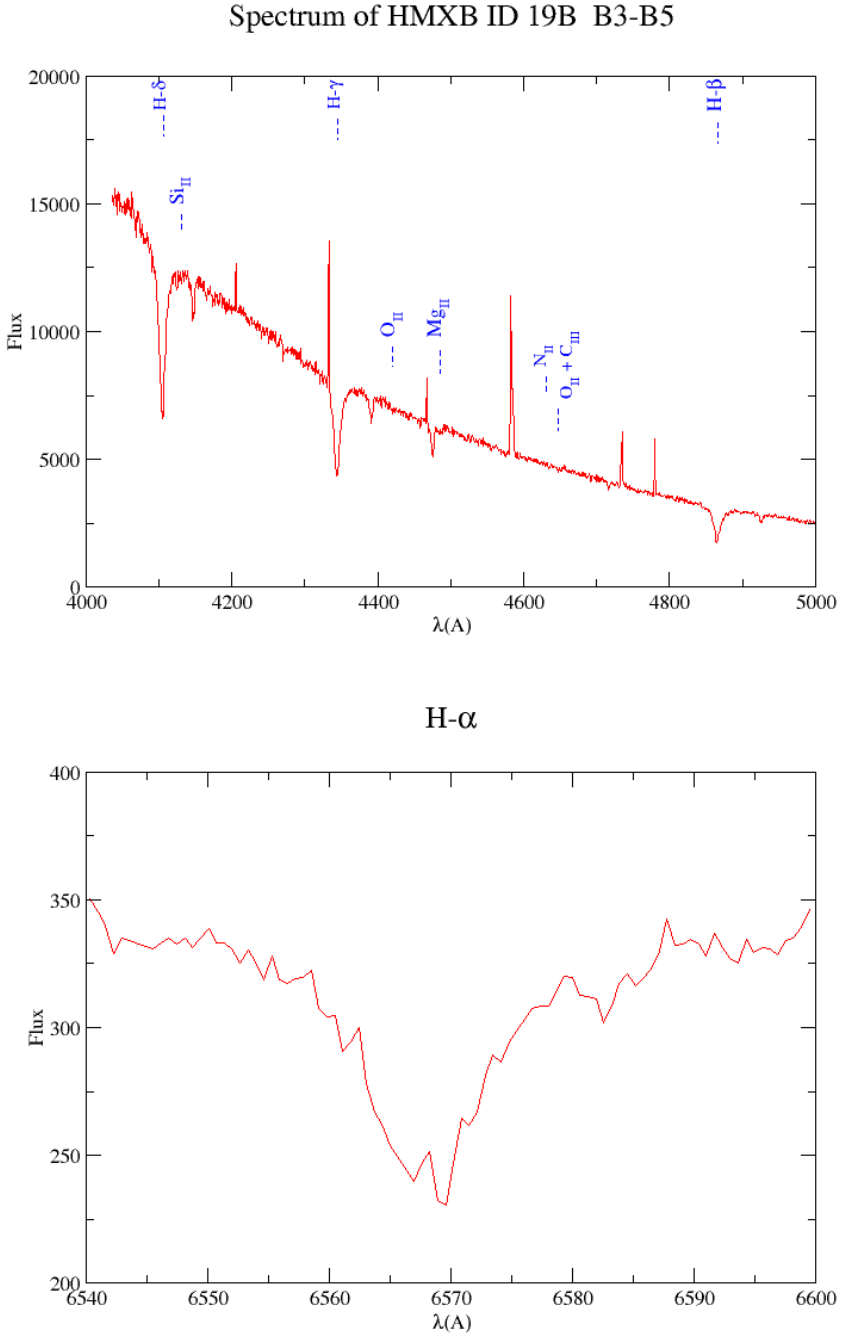

Figure 25: **Spectral regions for the blue part and H_α for the source ID:20**

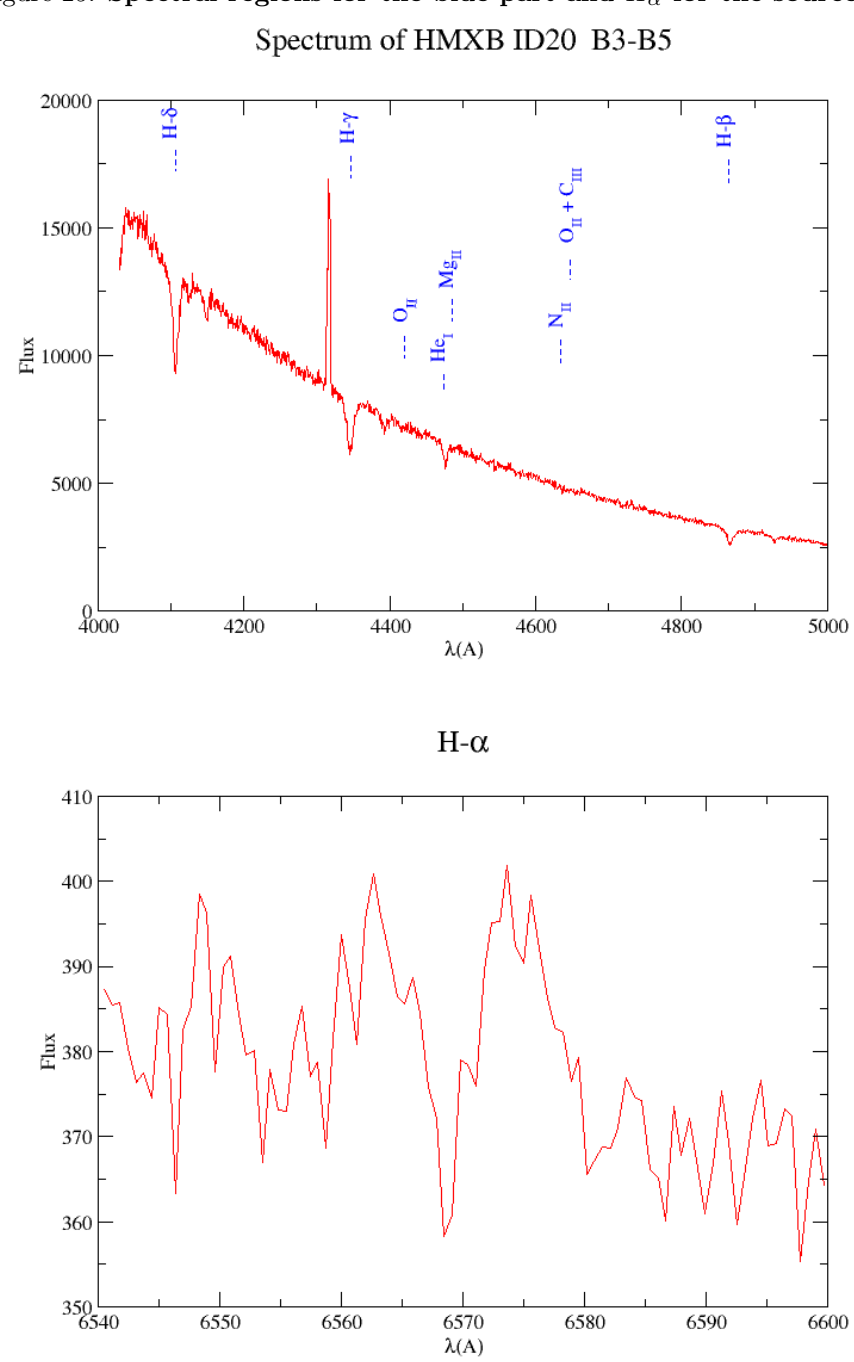

Figure 26: **Spectral regions for the blue part and H_α for the source ID:21**

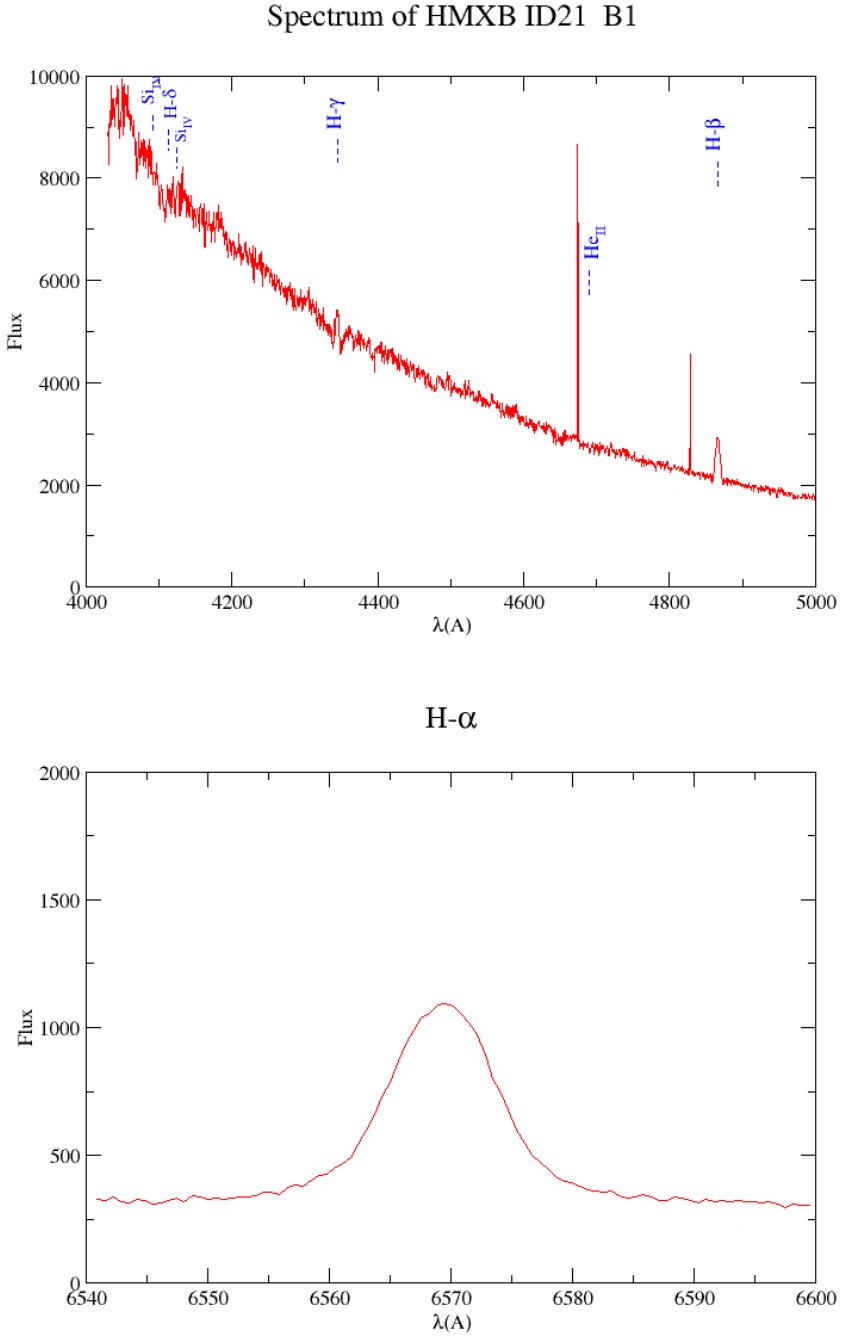

Figure 27: **Spectral regions for the blue part and H_α for the source ID:22**

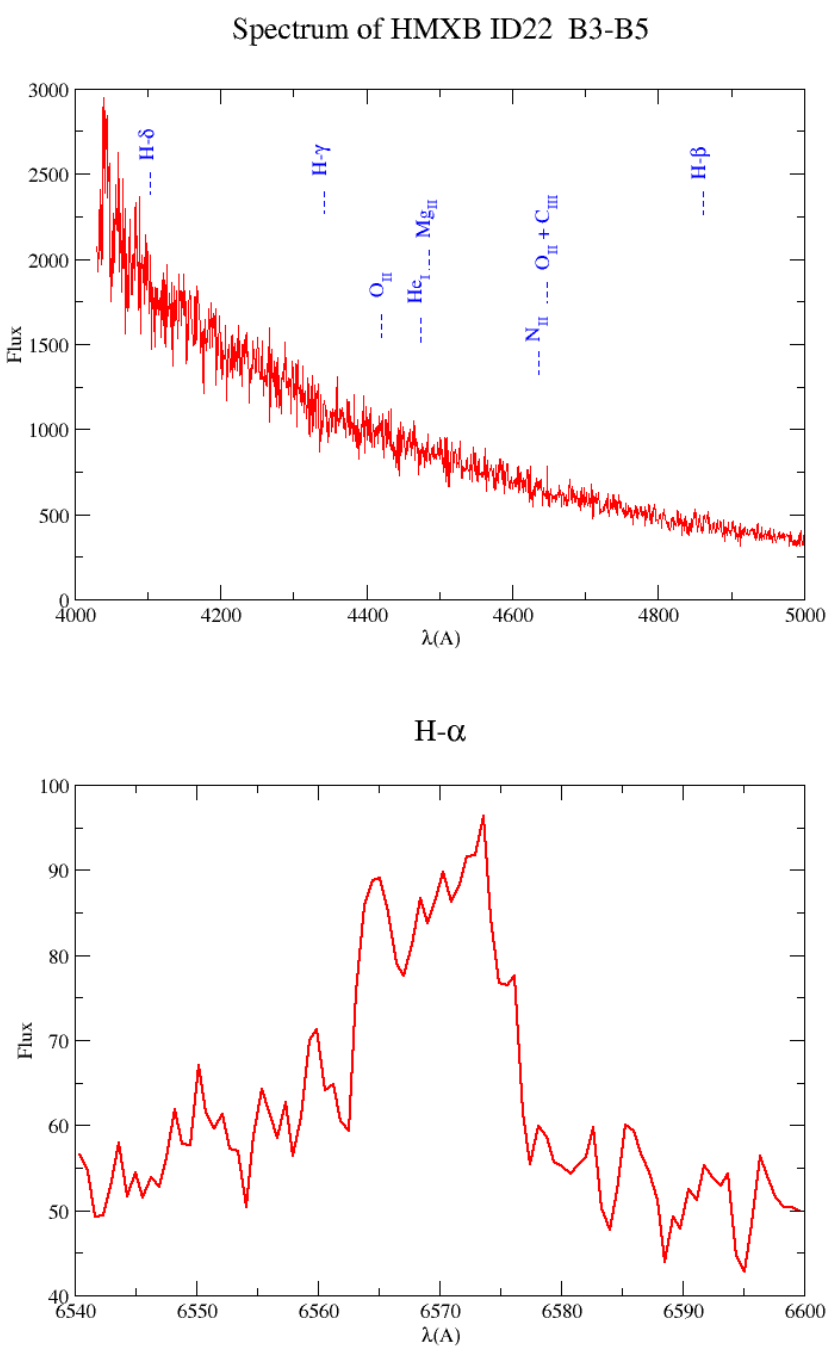

Figure 28: **Spectral regions for the blue part and H_α for the source ID:23A**

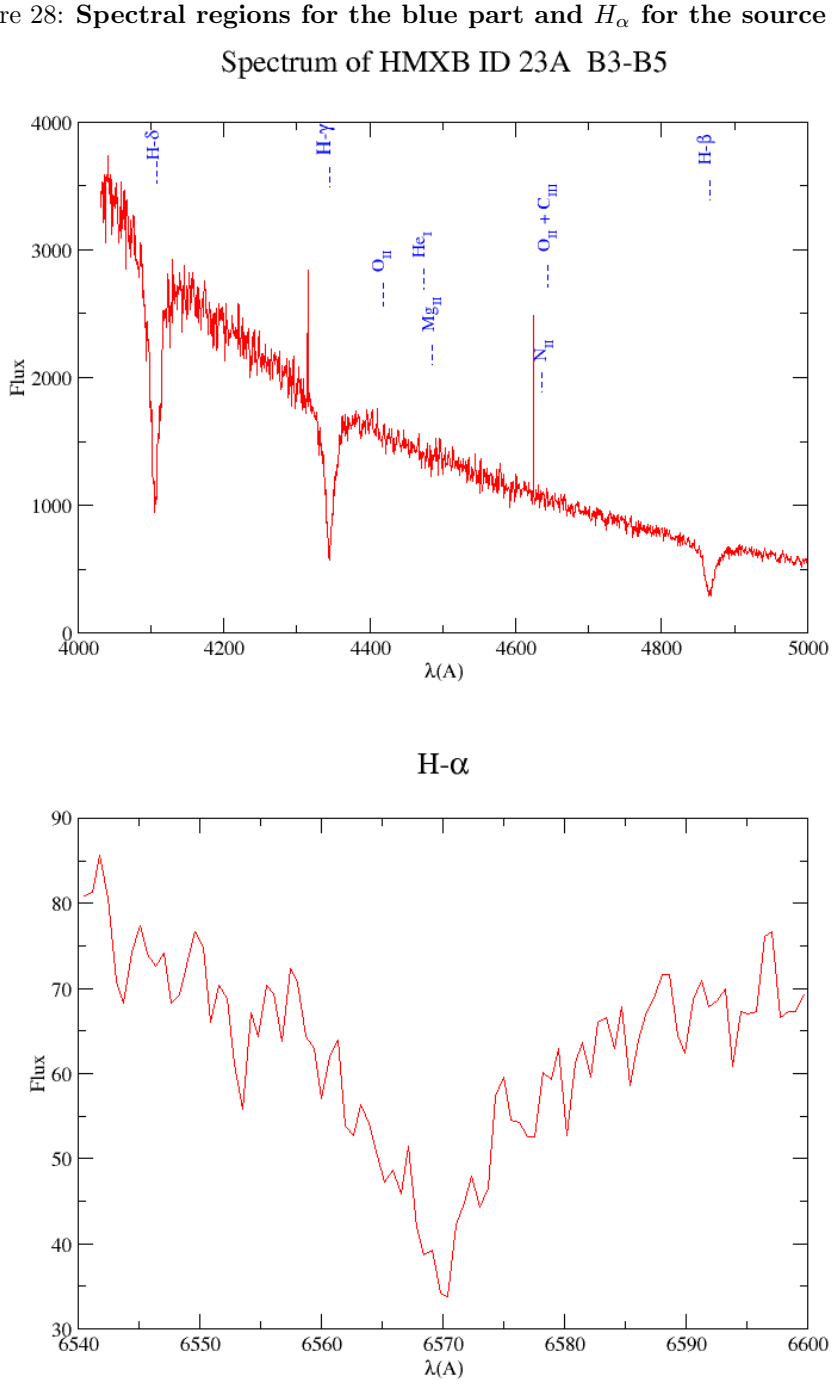

Figure 29: **Spectral regions for the blue part and H_α for the source ID:26**

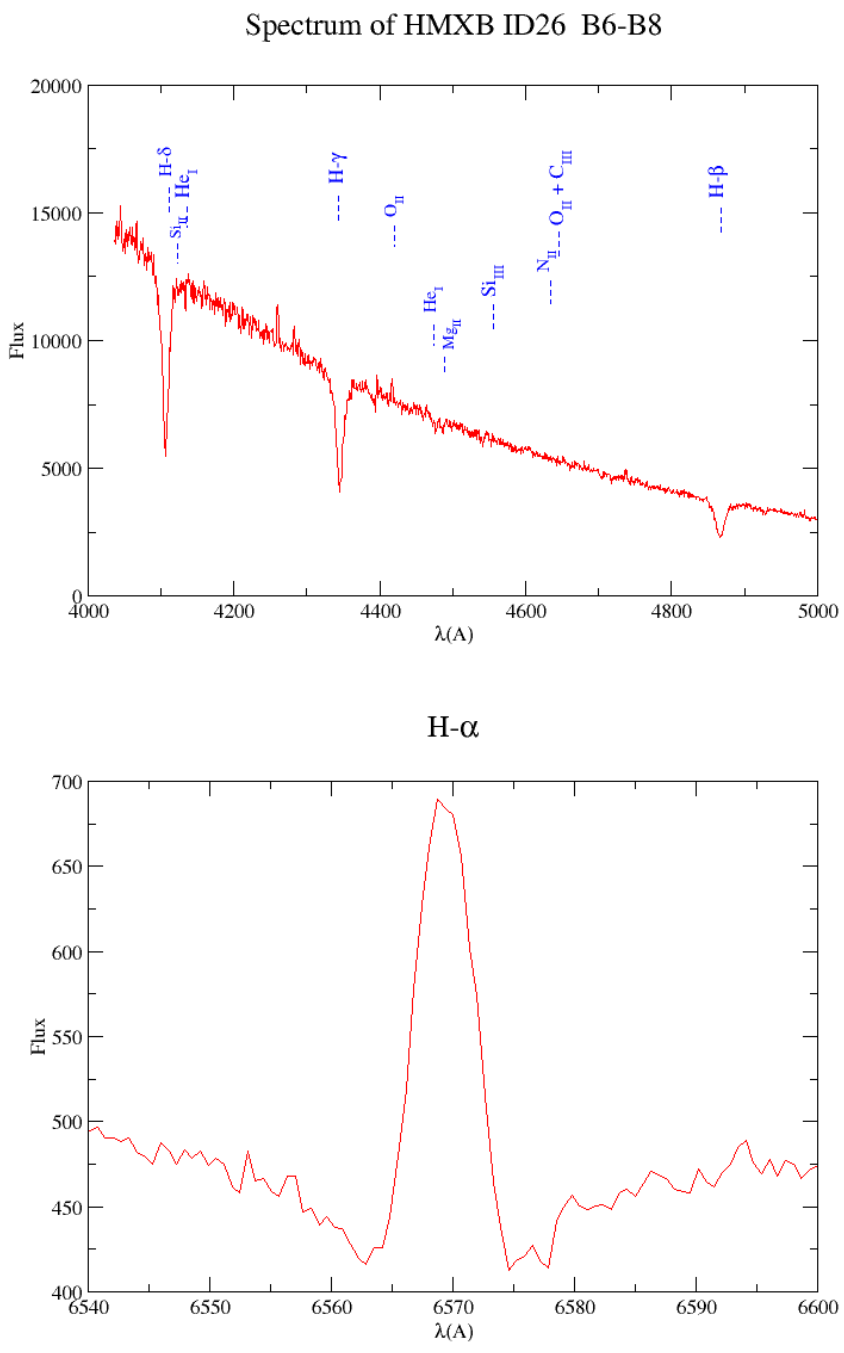

Figure 30: **Spectral regions for the blue part and H_α for the source ID:27**

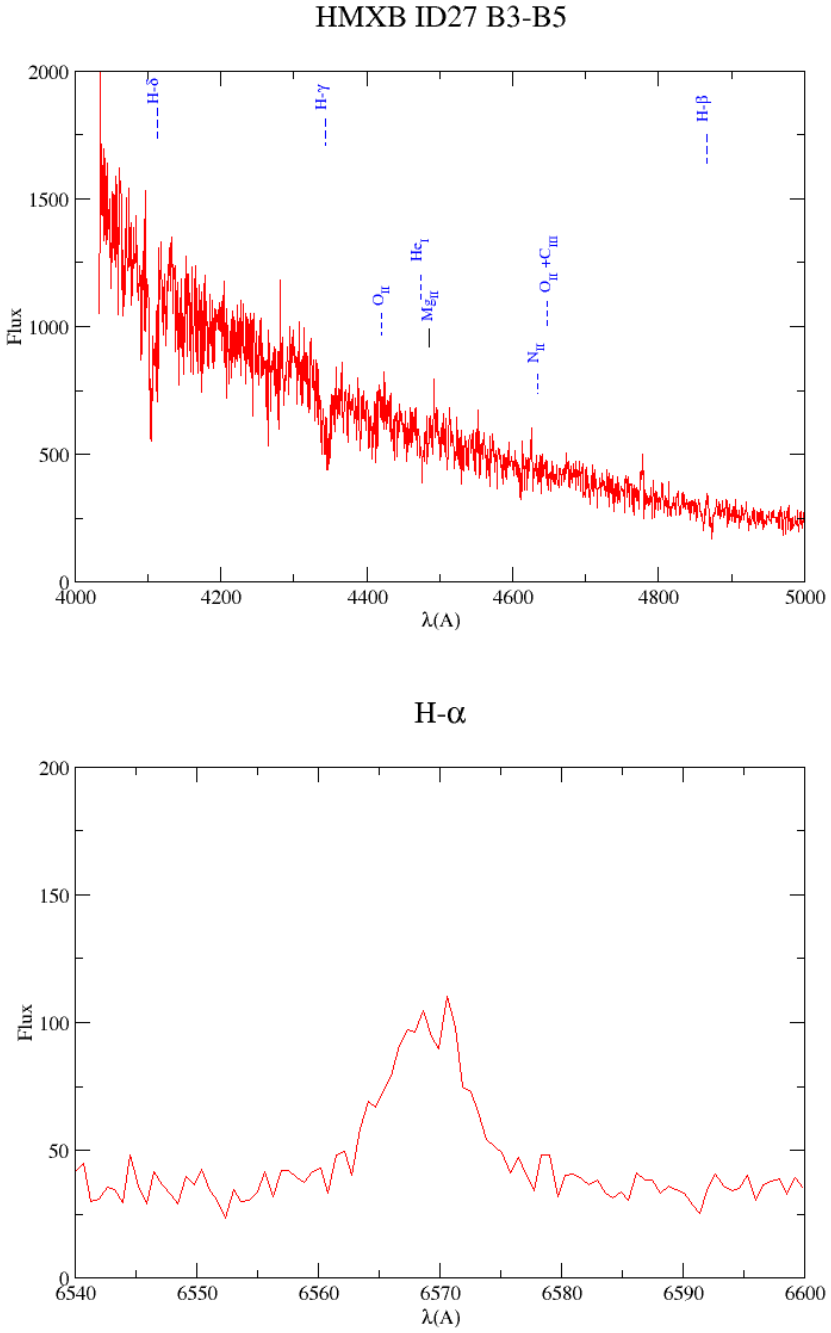

Figure 31: **Spectral regions for the blue part and H_α for the source ID:39B**

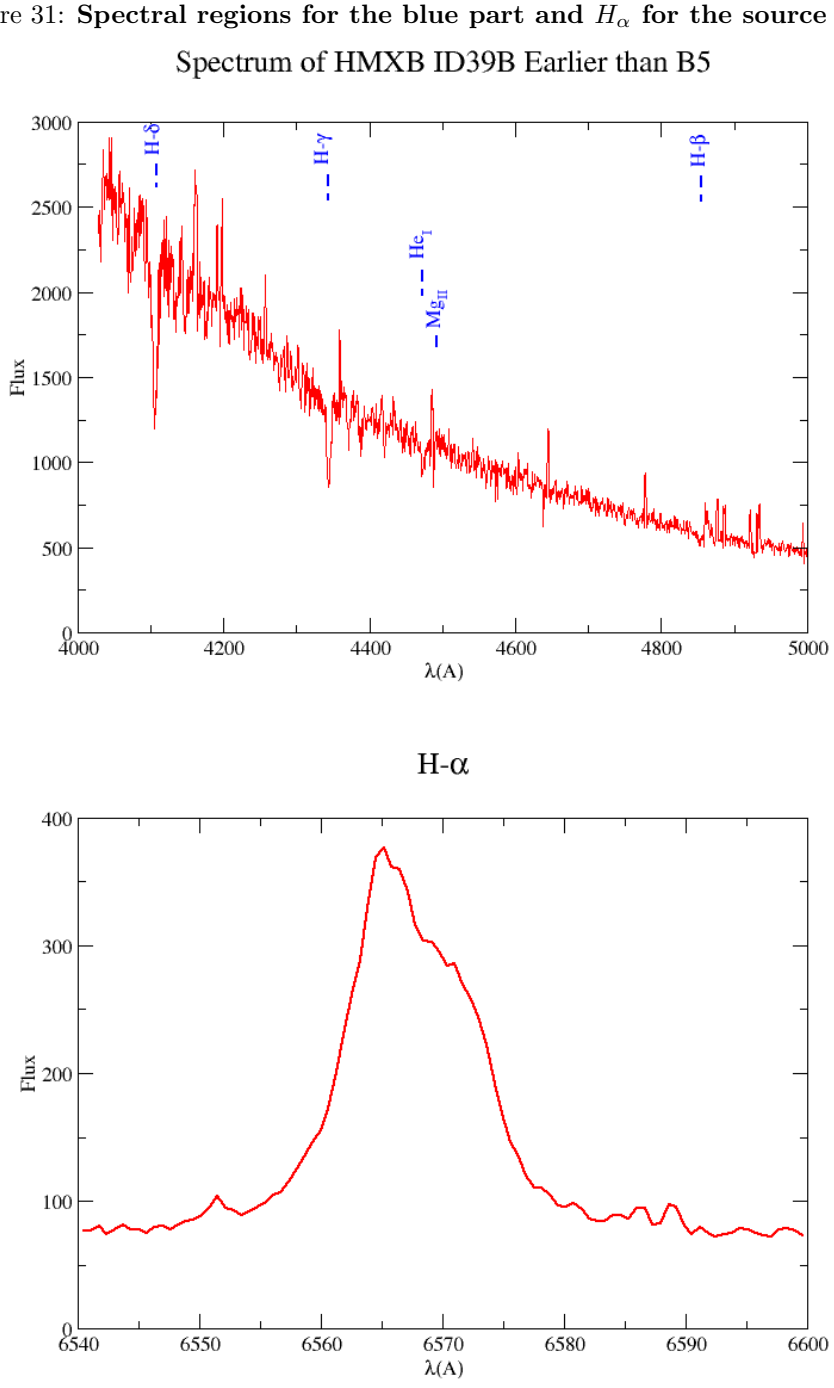

Figure 32: **Spectral regions for the blue part and H_α for the source ID:39C**

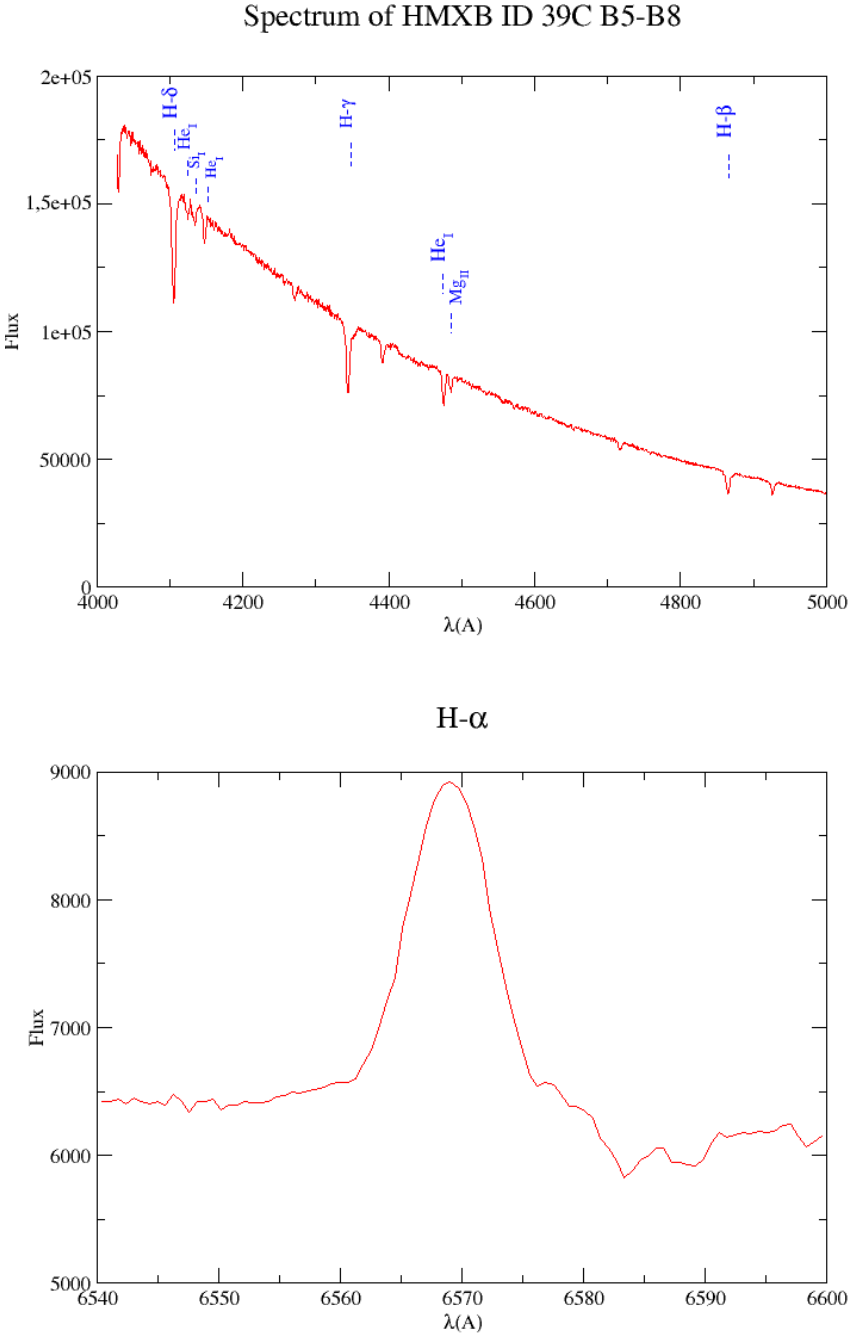

Figure 33: **Spectrum for the source ID:45B**

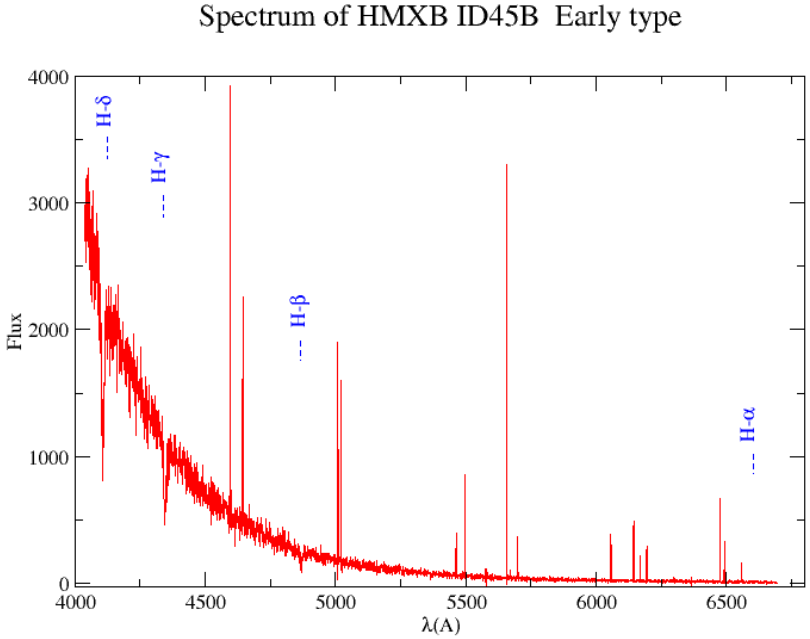

Figure 34: **Spectral regions for the blue part and H_α for the source ID:45C**

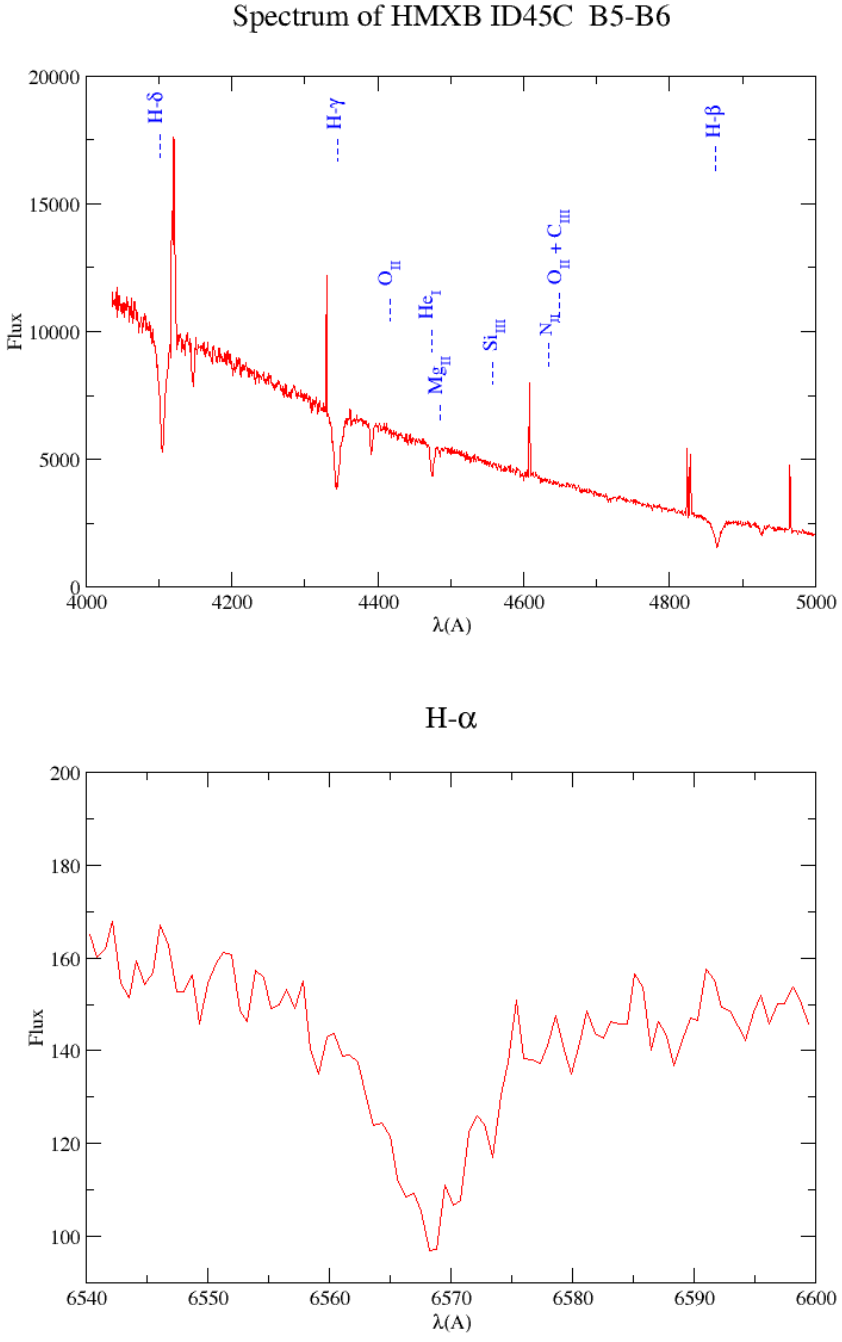

Figure 35: **Spectral regions for the blue part and H_α for the source ID:B**

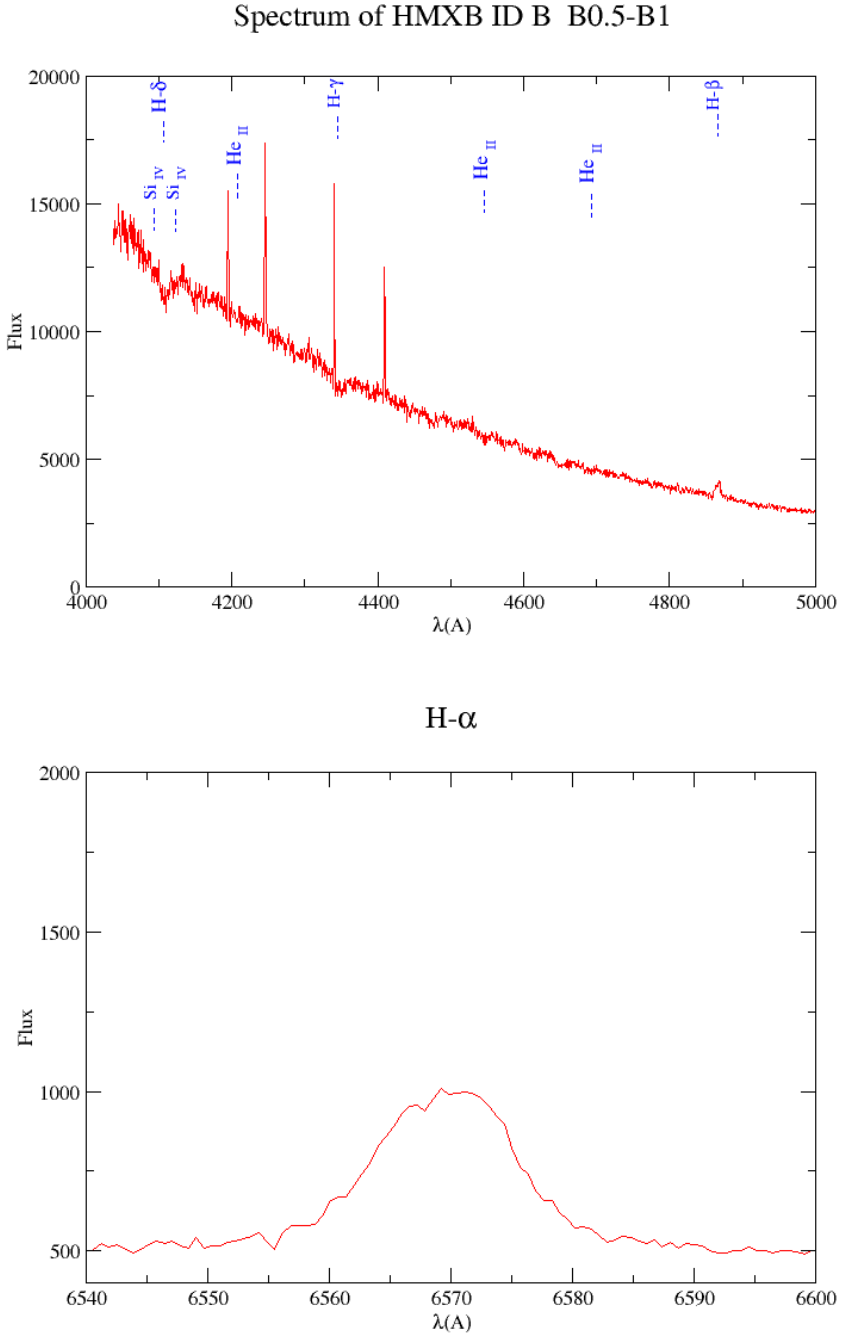

In Table 3 we present the final results. In column 1 we show the HMXB ID. In column 2 we present the previous classification of our objects and in column 3 our classification results. In column 4 we present the results about the the confirmation or not of our objects. As Confirmed Be star is characterized an object with early type spectral type and with Balmer lines in emission. As strong candidate is characterized an object with early type spectral type but with Balmer lines in absorption. Finally as tentative candidate is characterized an object with an indication of a early type spectral type but without any other clue for further classification.

Table 3: **Classification table**

HMXB ID	**Classification**		**Results**
	Antoniou,Zezas	This work	
(1)	(2)	(3)	(4)
3	-	Early Type (e)	Confirmed Be
4	-	B3-B5e	Confirmed Be
5	B2	B1-B1.5e	Confirmed Be
8	-	B8	Strong candidate
9	-	B3-B5e	Confirmed Be
10	-	B1.5-B2	Strong candidate
13	B0-B3e	B1	Confirmed Be
15A	-	Late Type	-
15B	-	Earlier than B5	Strong candidate
15C	-	B1.5	Strong candidate
16	-	O9e	Confirmed Be
17A	-	Late Type	-
19A	-	Later than B3	Strong candidate
19B	-	B3-B5	Strong candidate
20	B0.5e	B3-B5e	Confirmed Be
21	-	B1e	Confirmed Be
22	B0-B1.5e	B3-B5e	Confirmed Be
23A	-	B3-B5	Strong candidate
26	-	B5-B8e	Confirmed Be
27	B2(e?)	B3-B5e	Confirmed Be
39A	-	Early Type e	Tentative candidate
39B	-	Earlier than B5e	Confirmed Be
39C	B4	B5-B8e	Confirmed Be
45B	-	Early Type	Tentative candidate
45C	-	B5-B6	Strong candidate
B	-	B0.5-B1e	Confirmed Be

5.1 Discussion of individual sources

- ***HMXRB ID 4 : Classified as B3-B5***. The clear presence of a deep He_I $\lambda 4471$ absorption line and simultaneously the absence of Mg_{II} $\lambda 4631$ absorption line indicates a star with spectral type earlier than B5. The lack of $O_{II} + C_{III}$ $\lambda 4640 - 4650$ blend and the absence of N_{II} $\lambda 4632$ line means a spectral type later than B3. We cannot commet on the presence of the O_{II} $\lambda 4415 - 4417$ blend due to bad pixels. Thus we can suggest only a spectral type of B3-B5. The H_α $\lambda 6563$ exhibits a symmetric shell line profile which is indicative viwed edge-on. Depending on the line-of-sight we observe different line profiles.

If we observe a Be star edge-on the disk blocks part of th emission and leads to the formation of an absorption feayure ontop of the emission line, leading to the characteristic shell lines. On the other hand if we observe a Be star face-on we do not have any absorption (apart from the stellar surface) and the end result is a pure emission line.

- ***HMXRB ID 5 : Classified as B1-B1.5***.The presence of $O_{II}+C_{III}$ $\lambda 4640-4650$ blend indicates a star of spectral type earlier than B1.5. The He_{II} $\lambda 4686$ absorption line is absent. If the Si_{IV} $\lambda\lambda 4088, 4116$ are present the object will belong at the spectral type B1. The Si_{IV} $\lambda 4088$ is absent but for the Si_{IV} $\lambda 4116$ we have no information because of bad pixels. If we accept that Si_{IV} $\lambda 4116$ absorption line is absent and given that Si_{III} $\lambda 4553$ does not exist we can conclude that our star belongs to B1-B1.5 spectral types.All Balmer lines are in absorption.

- ***HMXRB ID 8: Classified as B8***. By comparison of the relative depth of absorption lines He_I 4121,$Si_I I$ $\lambda 4128-4132$ and He_I $\lambda 4144$ we see that He_I $4121 < Si_I I$ $\lambda 4128-4132$ $< He_I$ $\lambda 4144$. In addition Mg_{II} $\lambda 4481 < He_I 4471$. Thus, based on the criteria of a B8 star we suggest a spectral classification of B8.

- ***HMXRB ID 9 : Classified as B3-B5***.The clear presence of He_I $\lambda 4471$ and the absence of Mg_{II} $\lambda 4481$ indicates a star of spectral type earlier than B5. The $O_{II}+C_{III}$ $\lambda 4640-4650$ blend is absent. Also O_{II} $\lambda 4415-4417$ and N_{II} $\lambda 4631$ lines are absent. Thus, we can constrain the spectral type to B3 or later. Given tha lack of any more indicating lines we can only constrain the spectral type within the B3-B5 range. Regarding the Balmer lines, the H_α $\lambda 6563$ and H_β $\lambda 4862$ are in emission.

- ***HMXRB ID 10 : Classified as B1.5-B2***.Problem

- ***HMXRB ID 13 : Classified as B1*** The presence of $O_{II}+C_{III}$ $\lambda 4640-4650$ blend indicates a star of spectral type earlier than B1.5.The absence of He_{II} $\lambda 4686$ absorption line and the presence of Si_{IV} $\lambda\lambda 4088, 4116$ indicate a star of spectral type B1. Moving towards later spectral types we can see that the absence of Si_{IV} $\lambda\lambda 4116$ and the appearence of the Si_{III} $\lambda 4553$ suggests a star of spectral type B1.5. In our spectrum the He_{II} $\lambda 4686$ is absent and the Si_{IV} $\lambda 4088$ is present. For the Si_{IV} $\lambda 4116$ we have no information because of a bad pixel althought we can reject a spectral type of B1.5 duo to the absence of Si_{III} $\lambda 4553$. Thus, we can conclude with a spectal type B1. Regarding the Balmer lines only H_α is in emission.

- ***HMXRB ID 15A : Classified as Late Type***. The spectrum for this source is very unusual for a star of O-B spectral type. We can not find any relative indicator line for the O-B classification and thus we classified it as a Late Type star.
- ***HMXRB ID 15B : Classified as Earlier than B5***. The clear presence of He_I at $\lambda 4471$ and the absence of Mg_{II} at $\lambda 4481$ indicate a star of spectral type earlier than B5. Due to our inability to observe more indicator lines at the blue part of this spectrum we classify this object as Earlier than B5.

- ***HMXRB ID 15C : Classified as B1.5***. The absence of Si_{II} λ4116 line and the presence of Si_{III} λ4553 indicates a star of spectral type B1.5 or later.The absence of Mg_{II} λ4481 means that it can not belong to spectal types later than B2. Thus, we suggest a spectral classification of B1.5. Balmer lines are all in absorption.

- **HMXRB ID 16 :** ***Classified as O9***. According to Evans et al 2004 for O9 stars: $\mathrm{He}_{II}\lambda 4200 \sim He_I\ \lambda 4143$. However these lines reside in the blue part of the spectrum where we are not able to determine their presence or not. Moving towards hotter stars (earlier O-types the He_{II} become stronger and for O8.5 we have $He_{II}\ \lambda 4541 \sim He_I\ \lambda 4387$. From our spectrum we see that the $He_I\ \lambda 4387$ line is slightly stronger than the $He_{II}\ \lambda 4541$. Given our inability to confirm the presence of $He_{II}\ \lambda 4200$ and $He_I\ \lambda 4143$ lines (to compare) we can restrict the spectral type to O9-B0. Moreover, according to the OB classification scheme by Gray and Corbally we notice that the blend of $O_{II}+C_{III}\ \lambda 4640-4650$ becomes stronger than the $He_{II}\ \lambda 4686$ after O9.5 which is not case in our spectrum (He_{II} is obviously stronger).Thus, we coclude to spectral classification of O9. $H_\alpha\ \lambda 6563$ is in emmision and all the other Balmer lines we notice that both $H_\alpha\ \lambda 6563$ and $H_{beta}\ \lambda 4862$ are in emission.

- ***HMXRB ID 17A : Late Type***.The spectrum for this source is very unusual for a star of O-B spectral type. We can not find any relative indicator line for the O-B classification and thus we classified it as a Late Type star.

- ***HMXRB ID 19A : Classified as Later than B3***. The absence of $O_{II}+C_{III}\ \lambda 4640-4650$ blend and the absence of $O_{II}\ \lambda 4415-4417$ and the $N_{II}\ \lambda 4632$ absorpions lines indicated a star of spectral type later than B3. Because of the bad quality of the blue part of the spectrum we can classified this object only as later than B3. Regarding the Balmer lines we can see that H_α is staring to has a small emission and the H_β too.

- ***HMXRB ID 19B : Classified as B3-B5***.The clear presence of $He_I\ \lambda 4471$ absorption line indicates a spectral type earlier than B5. The $O_{II}+C_{III}\ \lambda 4640-4650$ blend is absent and the $O_{II}\ \lambda 4415-4417$ and the $N_{II}\ \lambda 4632$ absorpions lines are absent. So all the criteria for a star later than B3 are completely fullfiled. Also the $Si_{II}\ \lambda 4128-4132$ absorption line is absent too. It is not clear if the $Mg_{II}\ \lambda 4481$ absorption line exists.Given tha lack of any more indicating lines we can only constrain the spectral type within the B3-B5 range.

- ***HMXRB ID 20 : Classified as B3-B5***. The clear presence of $He_I\ \lambda 4471$ and the absence of $Mg_{II}\ \lambda 4481$ suggests a star of spectral type earlier than B5. The absence of $O_{II}+C_{III}\ \lambda 4640-4650$ blend and of the absorption lines $O_{II}\ \lambda 4415-4417$ and $N_{II}\ \lambda 4631$ indicates a star of spectral type later than B3. Because of the lack of indicator lines for spectral types between B3 and B5 we suggest a spectral classification of B3-B5.

- ***HMXRB ID 21 : Classified as B1***.The absence of absorption lines of He_{II} at $4200, 4541, 4686$ indicate us that our star belongs to spectral types B0.5 or later. On the other hand the presence of the absorption lines of Si_{IV} at $\lambda 4088, 4116$. Thus,the criteria for a star of spectral type B1 is completely fullfiled. Balmer lines are all in emmision except of $H-\delta$ which is in absorption and it is filled with a small emission.

- ***HMXRB ID 22 : Classified as B3-B5***. The $He_I\ \lambda 4471$ absorption line is present but the $Mg_{II}\ \lambda 4481$ line is absent.So our star belongs to spectral types earlier than B5. The $O_{II}+C_{III}\ \lambda 4640-4650$ blend is absent. In addition the absorption lines $O_{II}\ \lambda 4415-4417$ and $N_{II}\ \lambda 4631$ are absent.This suggests a star of spectral type later than B3. Therefore, due to the lack of indicator lines for spectral types between B3 and B5 we suggest a spectral

type of B3-B5. All Balmer lines are in emission except on H_δ for which we do not be sure if exists in the spectrum.

- ***HMXRB ID 23A : Classified as B3-B5***.The absence of $O_{II}+C_{III}$ $\lambda 4640-4650$ blend and the absence of absorption lines O_{II} $\lambda 4415-4417$ and N_{II} $\lambda 4631$ supports a spectral type later than B3.For spectral types earlier than B5 a criterio is the clear presence of He_I $\lambda 4471$ and the absence of Mg_{II} $\lambda 4481$. In our spectrum the Mg_{II} $\lambda 4481$ is absent but the He_I $\lambda 4471$ is absent too. Because of the absent of other indicator lines which suggest a spectral type later than B5 as well as the lack of indicator lines for spectral types between B3 and B5 we suggest a spectral classification of B3-B5.All Balmer lines are in absorption.

- ***HMXRB ID 26 : Classified as B5-B8***.The Si_{III} $\lambda 4553$ absorption line is absent and Si_{II} $\lambda 4128-4132 > He_I$ $\lambda 4121$ indicative of a spectral type later than B5. Moving towards later spectral types we see that for a B7 star we have He_I $\lambda 4471 \sim Mg_{II}$ $\lambda 4481$. Althought we cannot say with safety that the above criterio is consistent with our spectrum. Thus, we can restrict the spectral type to B5-B8. H_α line is in emmision.

- ***HMXRB ID 27 : Classified as B3-B5***. The He_I $\lambda 4471$ absorption line is present but the Mg_{II} $\lambda 4481$ line is absent.So our star belongs to spectral types earlier than B5. The $O_{II}+C_{III}$ $\lambda 4640-4650$ blend is absent. In addition the absorption lines O_{II} $\lambda 4415-4417$ and N_{II} $\lambda 4631$ are absent.This suggests a star of spectral type later than B3. Therefore, due to the lack of indicator lines for spectral types between B3 and B5 and with a sense of doubt because of the inability to observe more indicator lines at the blue spectral region we suggest a spectral type of B3-B5. Regarding the Balmer lines, H_δ and H_β are in emmision.

- ***HMXRB ID 39B : Earlier than B5***. The quality of the blue part of this source is not so good. Given our inability to recognize the indicator lines for a more strict classification and the fact tha we see the clear presence of He_I $\lambda 4471$ and the absence of Mg_{II} $\lambda 4481$ we suggest a spectral type earlier than B5. The H_α is in a strong emission.

- ***HMXRB ID 39C : Classified as B5-B8***.The clear presence of He_I $\lambda 4471$ and of Mg_{II} $\lambda 4481$ supports a spectral type later than B5. Also we clearly see that He_I $\lambda 4121 < Si_{II}$ $\lambda 4128-4132 < He_I$ $\lambda 4144$ and Mg_{II} $\lambda 4481 < He_I$ $\lambda 4471$. Due to the lack of indicator lines between spectral types B5-B8 we can classify our star as a star of spectral type B5-B8. H_α is in emission.

- ***HMXRB ID 45B : Classified as Early type***. The quality of the blue part of the spectrum does not allow us to classify with a specific spectral type or a specific spectral range this object. So due to the presence of Balmer lines we can say that it belongs to Early type spectral types. In addition we observe that H_α looks to be neither in absorption or emmision and H_β has a small emmision.

- ***HMXRB ID 45C : Classified as B5-B6***.The absence of $O_{II}+C_{III}$ $\lambda 4640-4650$ blend suggests that our star belongs to spectral types later than B3.In addition O_{II} $\lambda 4415-4417$ and N_{II} $\lambda 4631$ absorption lines are both absent as well as the Si_{III} 4553 and Si_{II} $\lambda 4128-4132$. On the other hand because of a bad line at $\lambda 4121$ we do not know if He_I $\lambda 4121$ exists.So we can not use surely the criterio for stars of spectral type B5.By visual examination of the appropiate spectra which we use as indicators we can say that for

spectral types B7 and later the $Mg_I I$ λ4481 becomes almost equal with He_I λ4471 and bigger than He_I λ4471 for later types (i.e. B9). In our case we have that $Mg_I I$ λ4481 $<$ He_I λ4471 . Thus we can restrict our spectral range between B5-B6. Balmer lines are all in absorption.

- ***HMXRB ID B : Classified as B0.5-B1***.According to the classification table the presence of $He_{II}\lambda$4686 and the absence of $He_{II}\lambda\lambda 4200, 4541$ would indicate a source of B0.5.On the other hand the presence of Si_{IV} $\lambda\lambda 4088, 4116$ and the absence of He_{II} λ4686 suggests a spectral type of B1. Given the lack of the He_{II} $\lambda\lambda 4200, 4541$ and the presence of He_{II} λ4541 we opt to assign a more conservative range of B0.5-B1.For the Balmer lines the H_α and H_β are in emission. H_γ and H_δ are both in absorption but the H_γ is filled in with some emission.

6 Discussion

In total we had 20 candidates HMXBs 14 of which are without previous classification. All of them had one optical counterpart except on HMXB ID:15,19,39 and 45 which had more than one optical counterparts. More specifically we had 3 canditates optical counterparts for HMXB ID 15:A,B,C, 2 for HMXB ID 19:A,B, 3 for HMXB ID 39: A,B,C and 2 for HMXB ID 45 :C,B. So finally we obtained the spectrum of 26 objects.
After the data analysis we concluded that from the 14 candidate HMXBs without previous classification 7 are confirmed BeXRBs 7, which means that the optical counterpart in each binary has an Early type spectral type and Balmer lines in emission. In most cases the $H-\alpha$ is in emission but there are objects with more than one Balmer lines in emission. 6 are characterized as strong candidates which means that their optical counterparts have an early type spectrum but not Balmer lines in emission and 1 characterized as a late type star.

6.1 Comments on HMXBs with more than one optical counterparts

- ***HMXB ID15:*** This HMXB has 3 cadidates optical counterparts A,B C. From the classification was obtained that A has a Late type spectral type and B classified as Earlier than B5. Finally C classified as B1.5. Thus we can reject with safety from the cadidates list the A an we suggest new observatios for B in order to obtain a more accurate classification while for C to detect possible emmision at a different epoch.

- ***HMXB ID17:***This HMXB has 3 cadidates optical counterparts A,B C.From the classification was obtained that A has a Late type spectral type and thus we can reject it with safety from the cadidates list. The other two optical candidates were not observed on this set of observation so we suggest new observations only for these two objects.

- ***HMXB ID19:***This HMXB has 2 cadidates optical counterparts A,B. From the classification was obtained that A is later than B3 while B is B3-B5. Thus we suggest new observatios for A in order to obtain a more accurate classification while for B to detect possible emmision at a different epoch.

- ***HMXB ID23:*** This HMXB has 2 candidates optical counterparts A B. We classified it as B3-B5 spectral type but with out Balmer lines in emission. So we can say that it is a strong candidate.The B was not observed on this set of observations so we suggest new observations for this object.

- ***HMXB ID39:***This HMXB has 3 cadidates optical counterparts A,B C. The A is a strong candidate because it has an Early type spectral type and $H-\alpha$ in emission. The B C have confirmed both as Be stars. Thus , because we are not sure which is the correct optical counterpart we suggest new observations for all the candidates with better resolution.

- ***HMXB ID45:*** This HMXB has 4 candidates optical counterparts A,B,C D. The A and B were not observed on this work. The B is characterized as an early type without Balmer lines in emission. So it is a tentative candidate. Finally C was classified as B5-B6 but also without Balmer lines in emission. Consecuently we suggest new observation for all the optical counterparts.

6.2 Comparison with previous classifications

- ***HMXRB ID 5 :*** The previous classification of this object was B2 III (Masetti et al,2006). From this the classification obtained as B1-B1.5e. Thus we can say that we are consistent with the previous classification but in our work we had better resolution than Masseti et al,2006).

- ***HMXRB ID 13 :***The previous classification of this object was B0-B3IIIe (Kahabka et al,2006) and obtained from Black-Body fits without considering spectral characteristics of the object. Our classification suggests a B1 spectral type and we can say that we are more accurate.

- ***HMXRB ID 20 :*** Haberl et al ,1997 suggested a spectral type of B2 ranging from B1 to B3.Their wavelength range is from 4500-6700 with smaller resolution and S/N ratio than our spectrum. Our spectrum allow us to improve this classification as B3-B5 source. However Negueruela et al,2002 obtain a spectrum of this source at a similar resolution but with less noise in blue part that allowed them to identify lines that we are not able to see in our spectrum (e.g He_{II} λ4686 and Si_{IV} λ4089). Thus their classification as B0.5 seems more accurate than our us.

- ***HMXRB ID 22 :*** Vasilopoulos et al,2013 suggested a spectral type B0-B1.5 based on the clear presence of spectral lines such as He_{II} λ4686, $O_{II}+C_{III}$. In our case we do not see these lines so we can only classify this object as B3-B5 possibly due to the low S/N ratio (~ 11)

- ***HMXRB ID 27 :*** Negueruela et al,2002 tentatively classified this source as B2 based on the relative ratios of HeI lines ,the strength of Mg_{II} λ4481 line , and the absence of any Si_{III} lines. In our case the proposed classification as B3-B5 is driven by the comparison of $He_I\lambda$4471 line to the $Mg_{II}\lambda$4481 line as the other lines are not obvious.

- ***HMXRB ID 39 :*** Sasaki et al,2000 suggested a spectral type of B2SG based on simple cross-corellation of the X-ray source to data bases (TYCHO ,DSS and SIMBAD).Farina et al,2009 performed a spectroscopic study of N159/160 complex in LMC where they detect the optical counterpart 39C(in our case) as star 158 (in their catalog) with a spectral classification of B4. We have assinged a spectral type of B5-B8 which is relatively consistent. As far as the other candidates 39A and 39B they do not provide any spectra so our analysis is the first to identify their early type nature (although more observations are needed to confirm their spectral types.)

As a conclusion we have 4 cases for which within one spectral subtype we are consistent with previous results. For the 2 cases (ID:20,22) we find later types (B3-B5) probably as a result of poor S/N ratio in the blue part of the spectra which hinder us from obtaining more accurate classification.

6.3 The HMXBs distribution in the LMC and the SMC

The recent census of HMXBs in the LMC suggests 23 confirmed HMXBs. With this work we can extend this sample to 30 confirmed HMXBs. In Figure we show the distribution which obtained from our sample in comparison with the previous sample from Antoniou Zezas,2016(5) and in comparison with the SMC sample from Maravelias et al,2014(8).

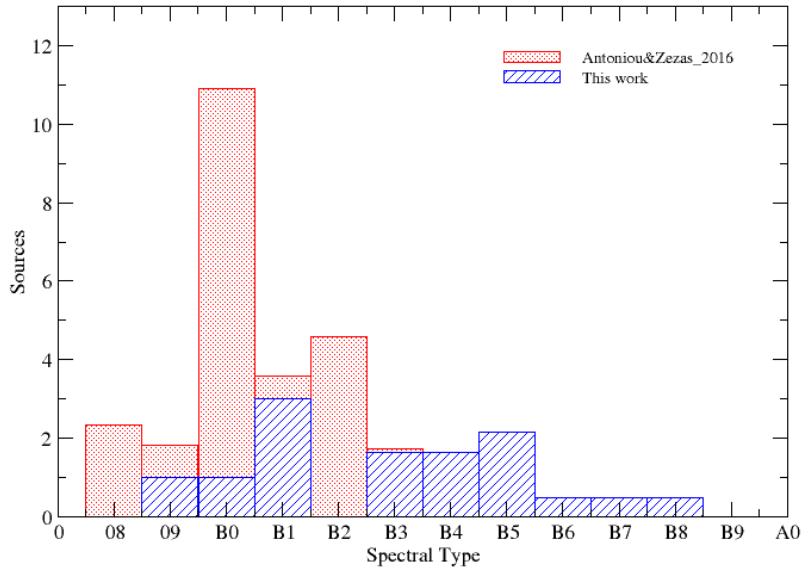

We see a lot of sources as B3-B5. That obtains from the bad blue part of the spectrum that we have in our observations. In general we need better resolution for the blue part in order to recognize more indication lines which classify a early type star.

References

[1] http://www.ctio.noao.edu

[2] http://www.iraf.noao.edu

[3] Giacconi,H.Gursky,H.,Paolini,F.R., Rossi,B.B. 1962,PRL,9,439

[4] Liu,Q.Z., van Paradijs, J. van den Heuvel, E.P.J. 2000, AASS,147.25.

[5] V.Antoniou and A.Zezas,2016, MNRAS.

[6] Pablo Reig,2011,Be/X-ray binaries

[7] Grigoris Maravelias,PHD Thesis,2014,"Investigation of the High-Mass X-ray Binary populations in the Small Maggelanic Cloud"

[8] G.Maravelias et al,2014,MNRAS,438,3,p. 2005-2025

[9] Chaty et al, 2011, ASP,447,p.29

[10] B.P. Abbott et al.(LIGO Scientific Collaboration and Virgo Collaboration), 2017, PRL,119, 161101

[11] Belczynski Ziolkowski, 2009,AsJ,707,2

[12] Okazaki et al, 1996,PASJ,48,305-315

[13] Bonfini Paolo-IRAF guide to Spectral Reduction

[14] Hilditch, R. W., Howarth, I. D., Harries, T. J. 2005, MNRAS, 357, 304 16, 24,42,111
ńskiński

[15] Pietrzyński et al.,2013,Nature, 495,76,16